Stress field changes in Central Europe from Late Miocene to Quaternary as determined from volcanic rocks in the Bohemian Massif

J. Stemberk Jr.[1,2], M. Coubal[1,3], and P. Štěpančíková[1]

[1]Institute of Rock Structure and Mechanics, The Czech Academy of Sciences, V Holešovičkách 94/41, Prague 8, 18000, Czech Republic.

[2]Faculty of Science, Charles University, Albertov 6, Prague 2, 12800, Czech Republic.

[3]Institute of Geology, The Czech Academy of Sciences, Rozvojová 269, Prague 6, 16000, Czech Republic.

Corresponding author: Jakub Stemberk (jakub.stemberk@irsm.cas.cz)

Key Points:

- Redefined timing of stress field changes since the Late Miocene in the W & N European Alpine foreland based on striae in dated volcanic rock
- New compressional and extensional stress regimes were discovered postdating 3.83 Ma
- Defined the behavior of the Sudetic Marginal fault and the Biala fault since Late Miocene to Quaternary

Abstract

This work presents the results of a paleostress investigation in dated Mio-Pliocene volcanic rocks in the vicinity of the town of Lądek Zdrój in the Rychlebské hory Mts., as a part of the central Sudetic Mts. in the NE Bohemian Massif. Six different paleostress field regimes from the Late Miocene to Quaternary were distinguished. Each stress regime is characterized by the orientation of the principal parameters and is discussed in relation to the known paleostress regimes within the surrounding regions of the Sudetic Mts., Fore-Sudetic block, and European Alpine foreland in Central Europe. The results show switching of tectonic phases with dominant compression, transtension or extension. Moreover, the orientation of theoretical planes with maximum shear stress and with a high tendency to dilate for individual paleostress regimes is defined and compared with the orientation of known faults within the study area suggesting their possible kinematics. The timing of the derived regimes is determined more accurately and is in good accordance with the data reported from different regions in Central Europe, which suggests their broader validity. In addition, one event or shorter events interrupting the main Plio-Quaternary extensional regime and one differently oriented Plio-Quaternary extension regime were discovered and constrained based on several dated phases of the volcanism of the faulted rocks.

1.1 Introduction

The Rychlebské hory Mts. (RH)/Złote Góry Mts. are situated in the NE part of the Bohemian Massif. They represent an aligned mountain ridge along the NW-SE striking Sudetic Marginal fault (SMF), which belongs to one of the most important faults in Central Europe (Badura et al., 2003; 2007; Ivan, 1966; Krzyszkowski et al., 1995; Oberc & Dyjor, 1969;

Štěpančíková et al., 2008; etc.). The SMF separates the relatively subsided Fore-Sudetic block in the NE, with the Sudetic Foreland (Fig. 1) formed by gently undulated relief with scattered groups of hills or slightly dissected uplands, from the elevated Sudetic block in the SW with the mountain ranges of the Sudetic Mts. with broad ridges and deeply dissected uplands and with an average elevation of 400-800 m a. s. l. (Štěpančíková & Stemberk Jr. 2016, Fig. 1). The Fore-Sudetic block is covered by a sequence of Miocene-Quaternary sediments (FSB, Fig. 6). The SMF zone was probably formed in the early Variscan and since the Permian it has moved mainly vertically (Pouba & Mísař, 1961). During the Alpine orogen cycle, the SMF was reactivated as a steeply-dipped normal fault with a horizontal component (Skácel, 2004). The neotectonic activity of the SMF has been studied intensively over the last decades (e.g. Badura et al., 2003; 2007; Danišík et al., 2012; Ivan 1966, 1997; Krzyszkowski et al., 1995; 2000; Oberc & Dyjor, 1969; Dyjor &Oberc, 1983; Skácel, 1989; Štěpančíková et al., 2008, 2010 and citations therein). The latest research suggests a diverse sense of slip on the SMF in different periods, but the present-day stress field is traditionally considered to have not changed since the Pliocene. Nevertheless, various authors assume a different sense of slip on the SMF since then. Dextral slip is inferred e.g. in Badura et al., (2007), whereas sinistral e.g. in Nováková (2010), Štěpančíková et al., (2008), Štěpančíková & Stemberk Jr. (2016), and possibly both senses of slip are inferred in Stemberk Jr., et al. (2019).

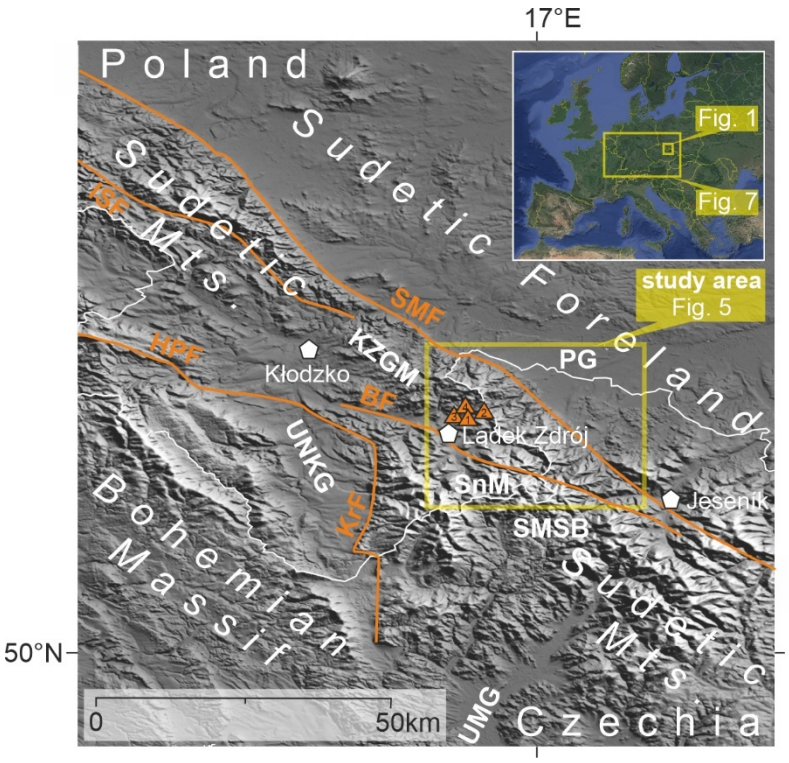

Figure 1. The topographic relief map of the Central Sudetic Mts. using SRTM (resolution 30m; Farr (Eds.), 2007) with the main fault zones and the main geological units. The Sudetic Marginal fault (SMF) forms a border between the Sudetic Mts. on the SW side and the Sudetic Foreland on the NE side. The main fault zones: BF – Biala fault zone; HPF – Hronov-Poříčí fault zone; ISF – Intra-Sudetic fault zone; KrF – Krowiarki fault zone; SMF – Sudetic Marginal fault zone. The main geological units: KZGM – Kłodzko-Złoty Stok granitoid massif; PG – Paczków

graben; SMSB – Staré Město shear belt. SnM – Śnieżnik massif; UMG – Upper Morava graben; UNKG – Upper Nysa Kłodzka graben.

The second important fault within the study area is the intra-mountain Bělský fault (BF), also known in Poland as the Biala, Bialawka or Trzebieszowice-Biala fault. Within the study area, the Biała Lądecka River follows the fault trend. It is a fault zone comprised of several subparallel and stepping fault segments striking NW-SE. Only a few authors have dealt with this fault system (e.g. Kasza, 1964; Ivan, 1966, Buday et al., 1997, Pospíšil et al., 2019). The BF zone continues to the SE through the Hrubý Jeseník Mts. and the Nízký Jeseník Highland as a step-over fault of the Sudetic Marginal fault and forms an 8 km-wide fault zone with CO_2 mineral springs in Karlova Studánka, and Dolní Moravice etc. (Hynie, 1963) and Neogene and Quaternary volcanos - Uhlířský vrch hill and Venušina sopka volcano. Historical (Guterch & Lewandowska-Marciniak, 2002; Pagaczewski, 1972) and present seismicity has also been documented in this area (e.g. Špaček et al., 2006; Zedník et al., 2001). To the NW of the study area, continuation of the BF is uncertain, but it probably continues across the Upper Nysa Kłodzka Graben (UNKG) and merges with the Intra-Sudetic fault zone (ISF) or the Krowiarki fault zone (KrF) and the Hronov-Poříčí fault zone (HPF; Fig. 1).

Due to the fact that the sense of slip on the faults is subjected to the orientation and parameters of the regional stress field (Fossen, 2010), the stress regime in the broader area has also been intensively studied by several authors during the last few decades. Data on tectonic processes were derived from knowledge of the geological and tectonic evolution (e.g. Ziegler, 1992; Dèzes et al., 2004; Ziegler & Dèzes, 2007), tectonostratigraphy (e.g. Meulenkamp et al., 2000a; 2000b; Sissingh, 2001; 2003; 2006; Rasser & Harzhauser et al., 2008), paleostress (e.g. Bergerat, 1987), volcanism (e.g. Merle & Michon, 2001), geomorphology (e.g. Badura et al., 2003), paleoseismology (e.g. Štěpančíková et al., 2010), seismology (e.g. Müller et al., 1992; Jarosiński, 2006) or extensometric measurements (e.g. Stemberk Jr. et al., 2019). Several stress field orientations were determined, but the age and time sequence of the suggested tectonic phases were not considered in detail. Nováková (2010) discovered four tectonic phases in limestone quarries near the town of Lipová Lázně. Jelínek (2008) suggested the Alpine rejuvenation of faults striking N-S to NNE-SSW and mainly W-E striking faults. Pešková et al. (2010) suggested two different tectonic phases: NE-SW compression and a transpressional tectonic regime for the Fore-Sudetic block, and NNW-SSE compression and a transtension tectonic regime since the Early Neogene for the Sudetic Mts. block. According to this work, the stress field has been more-or-less stable since the Miocene. Havíř (2002) reported WNW-ESE compression during the Neogene. The current stress field was determined by GPS measurements (e.g. Schenk et al., 2002; Kontny, 2004) as compression perpendicular to the strike of the SMF (~NE-SW compression). The current stress field was also computed by Havíř (2004), Vavryčuk et al. (2013) and Špaček et al. (2015) from focal mechanisms of micro earthquakes in broader areas as NW-SE compression. The switching of two stress/strain states based on extensometric measurements was reported by Stemberk Jr. et al. (2019) as WNW-ESE to NW-SE compression corresponding to the stress field of Western European and NNE-SSW compression corresponding to the stress field of the NW part of the Carpathian stress domain.

The paper deals with the Plio-Quaternary evolution of the Sudetic Mts., mainly within the study area in the RH. To determine the fault behavior in more detail, the paleostress field parameters were investigated on dated volcanic rocks. Based on the parameters of the determined

stress fields, theoretical fault planes with maximum shear stress and also theoretical fault planes with a tendency to dilate were determined and compared with known faults within the study area. These results and the determined orientations of the stress fields where compared to the stress fields discovered by several authors in the broader area of the European Alpine foreland and the Polish Lowlands basin since the Middle Miocene.

1.2 Geological setting

1.2.1 Structure geology and tectonics

The study area includes the Rychlebské hory Mts./Złote Góry Mts., which are situated in the Central Sudetes. The Sudetes represent the northeastern-most exposed fragment of the crystalline basement of the Variscan Belt in Europe, which is created by a variety of metamorphic complexes with Neoproterozoic, and Lower Paleozoic to Devonian protoliths (cf. Mazur et al., 2006; Kroner et al., 2008). They developed in the Devonian and Early Carboniferous as a result of closure of ocean basins and the amalgamation of Armorican terranes, followed by their accretion to the East European Platform (cf. Franke & Żelaźniewicz, 2000; Aleksandrowski & Mazur, 2002; Kroner et al., 2008). The Central Sudetes are geologically complex and consist of several units. The study area comprises the Śnieżnik massif unit (SnM) and borders the Kłodzko-Złoty Stok granitoid massif (KZGM) to the NW and the Staré Město shear belt (SMSB) to the SE (Fig. 1, Kroner et al., 2008). The Śnieżnik massif unit consists of augen orthogneiss, migmatites, gneiss, granulites and a stratigraphically higher Stronie unit with mica-schists and belts of crystalline limestone, amphibolite and quartzite, which originated from later Variscan tectonism (Aleksandrowski et al., 2000). Thermochronological data show the post-Variscan exhumation and unroofing in the studied part of the Central Sudetes to be ~7 km (Danišík et al., 2012). During the Late Cretaceous, the broader area was buried by the thick sedimentary cover (up to ~4–7 km) of the Cretaceous Sea and rapidly exhumed to near-surface temperatures during the Late Cretaceous-Paleocene. During the Paleocene and Eocene, the Sudetic and Fore-Sudetic blocks were elevated and eroded. The planated surfaces were partially covered due to Oligocene and Miocene marine transgressions coming from the Central European Basin (Oberc, 1972). The evolution of synsedimentary Paczków-Kędzierzyn (PG, Fig. 1; PKG, Fig. 5) and Roztoki-Mokrzeszowa grabens (RMG, Fig. 5) related to the SMF zone began to develop in the Latest Oligocene-Early Miocene (Dyjor & Oberc, 1983). The uplift of the Sudetic block with the formation of the Sudetic Mts. versus the Fore-Sudetic block began in the Pliocene, while the total uplift of the Sudetes since the Miocene has been estimated to be approximately 1200-1500 m. As a result, coarse syntectonic sediments of Gozdnica beds were deposited along the mountain front (Oberc, 1972; Dyjor & Oberc, 1983). The ensuing geological evolution of the study area is described in Chapter 5.

1.2.2 Volcanism

The Cenozoic volcanic activity in the broader area began in the Middle Oligocene and is divided into three volcanic phases (Birkenmajer et al., 1977). These phases indicate switching of compression phases and extension phases. The first phase occurred in the Middle Oligocene, the second phase occurred at the turn of the Oligocene and Miocene, and the third phase occurred from the Middle Miocene to the Pliocene. The volcano and its lava flows that originated during the third phase are situated in the vicinity of the village of Lutynia and Lądek Zdrój and were

dated by K-Ar and paleomagnetic methods as being 5.73-3.83 Ma (Birkenmajer et al., 2002; Cajz et al., 2012; Ulrych et al., 2013). Due to their Pliocene age, we have chosen them as being suitable for studying the Pliocene and younger paleostresses. The kinematic indicators were studied on four sites (Fig. 2, see Fig. 1 or Fig. 7 for their locations).

The **Čedičový vrch hill** site (CH, Fig. 2 - 2; N 50.35500°, E 016.92282°) is characterized as lava flows exposed in an old quarry on the main ridge of the Rychlebské hory Mts. (RH) approximately 3 km to the NE of Lądek Zdrój. A sequence of two lava flows is separated by a 2 m-thick layer of pyroclastic material. The volcanic rock has been classified as nephelitic basanite with olivines and xenoliths, which form volcanic columns (Fediuk & Fediuková, 1989). According to Ulrych et al., 2013, the age of lava flows is 5.73 Ma ± 0.23 Ma. To-date, measurement of a striae data set has only been performed in the uppermost 5-7 m thick lava flow.

The **Czerne Urwisko/Słupy Bazaltowe** site (CU, Fig. 2 - 4; N 50.36378°, E 016.90152°) is situated approximately 1.5 km to the NE of Lądek Zdrój near Lutynia. The rock has been classified as grey basanite rock, which creates a 15-20 m-thick lava flow, with subvertical volcanic columns that are 0.5–1 m in diameter. The rocks are exposed in an old pit and are from the Early Pliocene-Zanclean (3.83 Ma ± 0.17 Ma) according to K-Ar dating carried out by Birkenmajer et al. (2002).

The **Lutynia quarry** site (LQ, Fig. 2 - 1; N 50.35957°, E 016.91118°) is situated 2.5 km to the NE of Lądek Zdrój near Lutynia. It is presented as a volcanic plug dated to the Early Pliocene-Zanclean (4.56 Ma ± 0.20 Ma) after Birkenmajer et al., (2002). The site is an active quarry with walls 15-30 m high and volcanic columns 0.5 – 2 m in diameter.

The **Szary Kamień** site (SZ, Fig. 2 - 3a; N 50.35202°, E 016.8642°) is located approximately 1 km to the WNW of Lądek Zdrój. The lava flow is characterized as irregular volcanic columns, 0.5-1m in diameter and is exposed in an old pit. According to Berger (1932) and Walczak (1954), the basanite flow overlays fluvial gravels of the Biala Lądecka river terrace from the Pliocene or Early Pleistocene. Later research by Birkenmajer et al., (2002) using K-Ar

175 determined the age of the volcanic rocks as being from the Late Miocene – Messinian (5.46 Ma
176 ± 0.23 Ma).

177
178 **Figure 2**. The photomosaic of the volcanic rocks sites in Lutynia / Lądek Zdrój area. 1 – the
179 volcanic plug in the Lutynia quarry (LQ); 2 – the fragment of the lava flow on the Čedičový vrch
180 hill site (CH); 3a – the fragment of the lava flow on the Szary Kamień site (SK); 3b – example of
181 the slickenside with two sets of striae on the Szary Kamień site; 4 – the fragment of the lava flow
182 on the Czarne Urwisko site (CU).

183 ## 2 Methods

184 The volcanic rocks are intensively fractured in the all of the studied sites. Movement
185 along the fault planes is demonstrated by the presence of kinematic indicators (e.g. slickensides,
186 striae, calcite steps, stylolites, etc.). In this work, we collected kinematic information from
187 slickensides with striae (Fig. 2 - 3b). The datasets of striae on volcanic outcrops near Lądek
188 Zdrój and Lutynia with known radiometric K/Ar ages after Birkenmajer et al. (2002), Cajz et al.
189 (2012) and Ulrych et al. (2013) were used as input data for the application of paleostress
190 computational methods to determine the regional stress field characteristics during the Pliocene
191 and Quaternary.

192 ### 2.1 Parameters of the kinematic indicators

193 Each dataset from each site includes several measured kinematic characteristics of striae
194 on slickensides. They are described by two quantities: orientation of the fault plane with
195 components A_p (fault strike/trend), Φ_p (fault dip/plunge), and orientation of the striae with
196 component A_s (striae strike/trend), Φ_s (striae dip/plunge). Several measurements were
197 supplemented by the sense of slip on the plane (normal/reverse or sinistral/dextral). In some

cases, the slickensides contain multiple generations of striae. The superposition of these multiple generations of striae was also recorded (Sperner & Zweigel, 2010).

2.2 Analysis of the stress parameters

The paleostress analysis is based on continuum mechanics, which estimates the parameters of a slip on arbitrary slickensides for the known parameters of stress orientation (Angelier et al., 1982; Angelier, 1989). In practice, the inverse situation is solved where the principal parameters of the stress that caused the later measured slips on the slickensides recorded as striae are calculated from the measured slip orientation on several slickensides. The principal stress parameters are expressed as a total stress tensor. In this work, a reduced stress tensor was calculated, which approximates the total stress tensor neglecting the isotropic part of the crustal stress (Angelier, 1989, 1994). The approximation can be used because the site is located in very shallow parts of the Earth's crust.

Processing of the datasets consisted of two phases. During the first phase, all of the datasets from the individual sites were processed in the updated software ROCK2014 (Málek et al., 1991). This software automatically separates datasets of measured striae to statistic groups with similar parameters. It uses the polyphase analysis numerical method after Angelier (1994) to determine the stress field orientation from the kinematic characteristics of the individual striae. The misfit angle α (Tab. 1) between the observed striae on the slickenside and theoretical ones, which correspond to a computed stress state, was also calculated (Hippolyte et al., 2012). In this work, a misfit angle of less than 25° is assumed as a good agreement. A heterogeneous data set of striae is divided into homogenous subsets – paleostress states (e.g. SK-1, LQ-2, etc., Tab. 1, Fig. 3) based on a comparison of misfit angles with all of the individual stress states. The data distribution of misfit angles grouped into 5° intervals is presented on histograms in Fig. 3 and represents the quality indicator of the determined paleostress states. The reliability and precision of the method used are discussed in e.g. Coubal et al. (2015).

During the second phase, paleostress states were compared using an approximative method of P and T-axes in the FaultKin 7 software (cf. Marrett & Allmendinger, 1990; Allmendinger et al., 2012). Paleostress patterns (marked as PPA-PPF) were defined and visualized as stereo-plots (Fig. 4) and the stress field parameters presented in Tab. 2a and Tab 2b. The time aspect was also considered during the comparison.

The reduced stress tensor, which characterizes the single paleostress state/pattern, has the following principal parameters: direction of its principal stresses (σ1 – maximum, σ2 – intermediate and σ3 – minimum) and ratio $\Phi = (\sigma2-\sigma3)/(\sigma1-\sigma3)$ describing the difference between the magnitudes of the principal stresses (Angelier, 1994). The values of Φ range from 0 (uniaxial compression) to 1 (uniaxial extension). The Φ ratio parameter varies depending on the amount of data (n) in the individual paleostress state/pattern (Málek et al., 1991). Paleostress states/patterns with sub-horizontal σ1 were marked as compressional, and episodes with subhorizontal σ3 were marked as extensional (cf. Stemberk Jr. at al., 2019).

The determined stress field parameters were then used to determine the parameters of fault planes, where the normal component is the lowest and the shear stress component is the highest. According to the Coulomb stress criterion, these planes may have been activated by slips

during single paleostress patterns (Moriss et al., 1996; Fossen, 2010). There are two planes, with theoretical orientation ±45° from σ1 and transect in σ2. In practice, based on empiric observations, the angle between σ1 and both the planes is lower. In this work, we used as a good approximation of the value of angle ±30° (Ramsay & Huber, 1987; Fossen, 2010). Similarly, the planes that are perpendicular to the σ3 axis tend to dilate (Ramsay & Lisle, 2000) (Fig. 7). The computed theoretical fault planes (Fig. 4) were compared with published faults (fault segments with uniform strikes) within the study area in each paleostress pattern. The faults where collected from map sources: Don et al. (2003), Müller and Čurda (2003), Skácel (1989), Skácelová (1992a; 1992b; 1997), map portal of the Czech Geological Survey, geological maps of the Sudetes: 902C-Trzebieszowice (Cwojdziński, 1977), 902D-Lądek Zdrój (Gierwielanic, 1968), 934A-Stronie Śląskie (Cwojdziński, 1981) and 934B-Strachocin, Bielice (Cymerman & Cwojdziński 1984). Unfortunately, there is no detailed information about fault geometries, only about the strike. According to Skácel (1963) and Ivan (1966), most of the faults in the broader area are nearly sub-vertical, but the fault dip orientation and angle are unknown. We only approximated the issue of the reactivation of the faults to the distribution of the fault strikes, where the dip angle and dip direction were not considered. When the orientation of the fault differs less then ±10° from theoretical one, the fault was marked as a fault with a tendency to slip/dilate. A fault with a strike difference of ±5° from the theoretical one was marked as a fault with a high tendency to slip/dilate (Fig. 7).

Moreover, based on the mechanics (e.g. Angelier, 1994), the stress field causes the same sense of slip on all of the parallel faults at all of the different scales. The block diagrams in Fig. 4 show the determined slips on slickensides in volcanic rocks applied to a larger scale of relief evolution in the individual paleostress patterns.

The important aspect used in this work is the time-sequence of the determined paleostress patterns. The first method used is relative timing. This is based on the fact that the registered data contain a sequence of variously superimposed generations of striae on reactivated slickensides. The second method, sub-geochronological timing, is based on studying the kinematics of brittle structures and their relationships with geochronologically dated rocks. In this case, the Tertiary bazaltoid volcanic rocks dated by the K-Ar dating method carried out by Birkenmajer et al. (2002), Cajz et al. (2012) and Ulrych et al. (2013) were used. It is possible to suggest the time period of the paleostress pattern action based on whether it is disrupting volcanic rocks of different ages or not. The dating of volcanic rocks comes with certain inaccuracies, but in comparison with commonly used geological timing based on disrupting sediment formations, it is a significant refinement of the time periods.

3 Results

Based on the similarity of the stress tensor parameters and their time-superposition, six groups of paleostress patterns were identified and marked as PPA-PPF (Fig. 3; Fig. 4). The paleostress patterns are sorted chronologically. All of the presented paleostress patterns are from

the Late Miocene to Pleistocene. The age is estimated as an interval between the dated volcanic events (after Birkenmajer et al., (2002), Ulrych et al. (2013) and Cajz et al. (2012)).

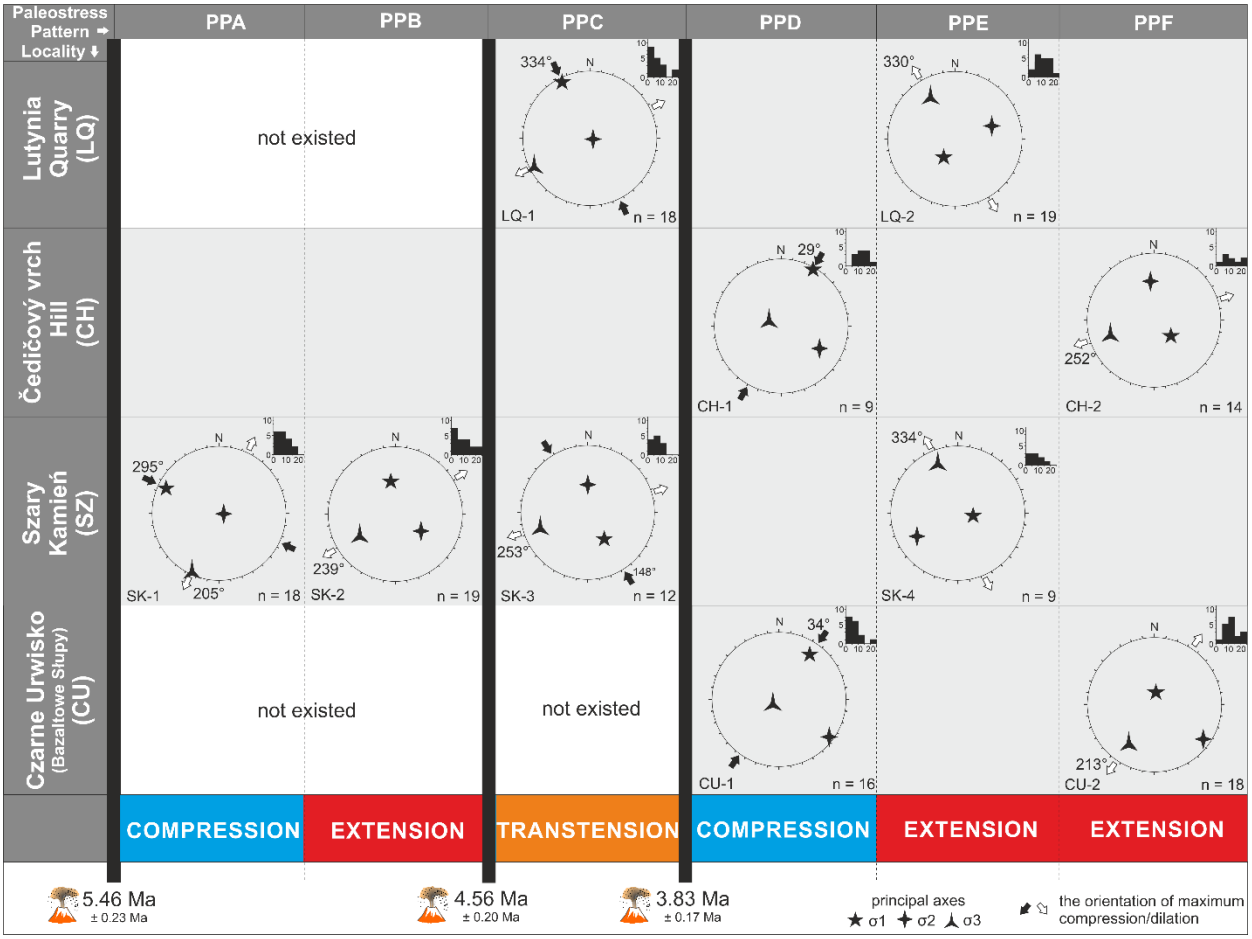

Figure 3. The paleostress states (e.g. CU-2) after the updated software ROCK2014 (Málek et al., 1991) and the paleostress patterns (e.g. PPA) sorted by sites in time sequence. The histograms in individual paleostress states show the data quality based on the misfit angle in range 0°-25°; n = sum of striae in the individual paleostress states.

Paleostress state	σ1		σ2		σ3		Φ	n	Q
	Tr.	Pl.	Tr.	Pl.	Tr.	Pl.			
CU-1	34°	32°	335°	29°	266°	40°	0.278	16	A
CU-2	15°	58°	121°	20°	213°	21°	0.698	18	A
CH-1	29°	1°	120°	23°	295°	67°	0.145	9	C
CH-2	132°	52°	355°	30°	252°	21°	0.848	14	B
LQ-1	334°	4°	103°	84°	243°	4°	0.775	18	A
LQ-2	213°	55°	71°	30°	330°	18°	0.638	19	A
SK-1	295°	8°	94°	82°	205°	3°	0.294	18	A
SK-2	148°	40°	0°	45°	253°	17°	0.288	19	A
SK-3	352°	38°	123°	41°	239°	27°	0.816	12	B
SK-4	100°	62°	241°	20°	334°	11°	0.756	9	C

Table 1. The parameters of the paleostress states. Tr. – trend; Pl. – plunge; Φ – the ratio of the stress differences Φ = (σ2- σ3)/(σ1- σ3); n – number of events forming homogenous subset; Q – quality estimator for the fault-slip data datasets. The grade of the quality estimator is based on the number of events forming the homogenous dataset: A – 15 or more events (excellent), B – 10-14 events (good), C – 4-9 events (fair), D – 4 events (poor) (after Coubal et al. 2015).

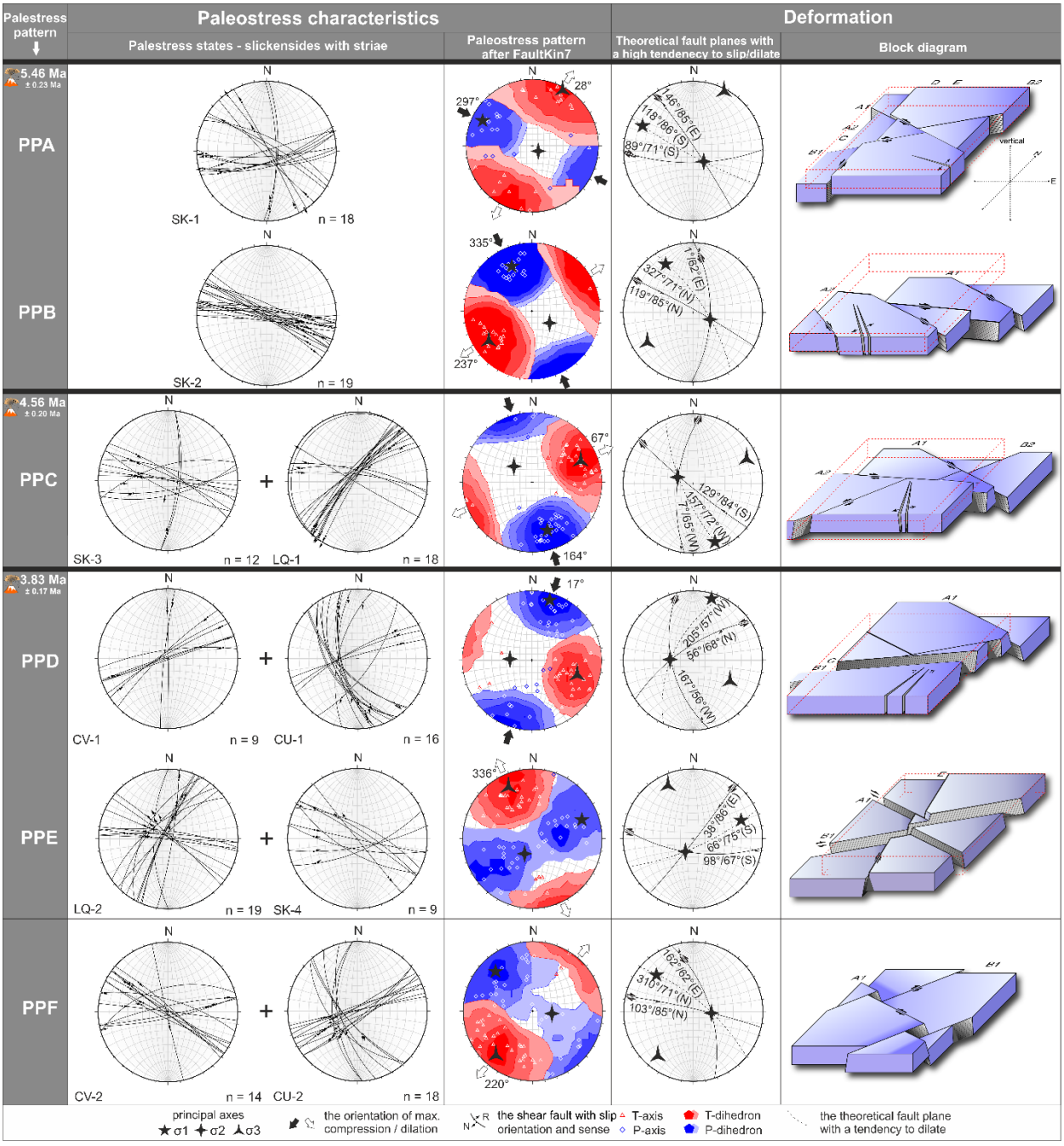

Figure 4. The results of the fault slip dynamics analysis. Overall character of the observed paleostress patterns. First column shows the stereo-plots of the slickensides with striae in the individual paleostress states (e.g. SK-1), which belong to the same paleostress pattern (e.g. PPA);

n = sum of striae on slickensides in the individual paleostress states. Second column shows beach ball charts of the P-axis and the T-axis orientation after the software FaultKin 7 (Allmendinger et al., 2012). Third column shows the stereographic plots with the planes with maximum shear stress/a high tendency to slip (after Ramsay & Huber, 1987; Fossen, 2010) and the planes/fissures with a high tendency to open (Ramsay & Lisle, 2000). Fourth column shows the block diagrams created based on the observed slickensides in the volcanic rocks and its deformation caused by the paleostress field action.

Paleo-stress pattern	σ1		σ2		σ3		n	Q	Included paleostress states
	Tr.	Pl.	Tr.	Pl.	Tr.	Pl.			
PPA	297°	17°	131°	72°	28°	4°	18	A	SK-1
PPB	335°	22°	111°	60°	237°	19°	19	A	SK-2
PPC	164°	19°	296°	64°	67°	18°	30	A	LQ-1, SK-3
PPD	17°	11°	271°	55°	115°	33°	25	A	CH-1, CU-1
PPE	71°	18°	208°	66°	336°	15°	28	A	LQ-2, SK-4
PPF	319°	23°	94°	60°	220°	19°	32	A	CH-2, CU-2

Table 2a. The parameters of the paleostress patterns (part 1). Str. – strike; Tr. – trend; Pl. – plunge; N – normal; R – reverse; S – sinestral; D – dextral; n – number of events forming homogenous subset; Q – quality estimator for fault-slip data subset. The grade of the quality estimator is based on the number of events forming the homogenous subset: A – 15 or more events (excellent), B – 10-14 events (good), C – 4-9 events (fair), D – 4 events (poor) (after Coubal et al., 2015).

Paleo-stress pattern	Theoretical plane 1 with maximum shear stress		Theoretical plane 2 with maximum shear stress		Theoretical plane with a tendency to open
	Plane (Str./Dip)	Striae (Tr./Pl.)	Plane (Str./Dip)	Striae (Tr./Pl.)	Plane (Str./Dip)
PPA	146°/85° to E	327°/18° S/N	89°/71° to S	266°/13° D/N	118°/86° to S
PPB	1°/62° to E	5°/9° S/N	119°/85° to N	302°/30° D/R	327°/71° to E
PPC	129°/84° to S	132°/24° D/R	7°/65° to W	191°/7° S/N	157°/72° to W
PPD	56°/68° to N	45°/26° S/R	167°/56° to W	171°/6° D/R	205°/57° to W
PPE	38°/86° to E	40°/23° D/R	98°/67° to S	101°/7° S/N	66°/75° to S
PPF	103°/85° to N	286°/29° D/R	162°/62° to E	347°/10° S/N	310°/71° to N

Table 2b. The parameters of the paleostress patterns (part 2). Str. – strike; Tr. – trend; Pl. – plunge; N – normal; R – reverse; S – sinestral; D – dextral.

3.1 Late Miocene-Early Pliocene WNW-ESE compression - PPA

This compression phase was constructed based on a dataset containing 18 striae on slickensides, and was only identified at the Szary Kamień site as paleostress state SK-1 (Fig. 4). The compression must have appeared between 5.46 Ma ± 0.23 Ma and 4.56 ± 0.20 Ma. The orientation of the principal axes is subhorizontal σ1 (297°/17° after FaultKin7; trend/plunge) and subhorizontal σ3 (28°/4°). The set of planes with maximum shear stress is oriented subvertically 89°/71° (strike/dip) to the S as a dextral/normal fault and 146°/85° to the E as a sinistral/normal fault. The plane with the highest tendency to open is oriented subvertically 118°/86° to the S. This stress field configuration produced subsidence of the western blocks towards the eastern ones. The NW-SE to WNW-ESE oriented faults had a sinistral sense of movement with no

vertical component, and the WSW-ESE oriented faults had a dextral sense of movement, also without any vertical component. A block diagram with a schematic sketch of the block deformations is presented in Fig. 4.

3.2 Late Miocene-Early Pliocene NE-SW extension - PPB

This extension phase was reconstructed based on a dataset containing 19 striae on slickensides. It was only identified at the Szary Kamień site as a paleostress state SK-2 (Fig. 4). The extension must have appeared between 5.46 Ma ± 0.23 Ma and 4.56 ± 0.20 Ma (Late Miocene-Early Pliocene), following the previous phase. The orientation of the principal axes is σ1 335°/22° and σ3 237°/19°. The planes with the maximum shear stress are oriented 1°/62°to the E as a sinistral/normal fault and 119°/85° to the N as a dextral/reverse fault. The plane with the highest tendency to dilate has an orientation of 327°/71° to the E. This stress field has produced a complicated structure with uplifted northern blocks towards the southern ones. Moreover, the eastern blocks are subsiding against the western blocks separated by subvertical N-S trending faults. The faults striking WNW-ESE to WSW-ENE have a dextral sense of movement (see the block diagram in Fig. 4).

3.3 Early Pliocene transtension - ENE-WSW extension/NNW-SSE compression - PPC

This phase has no dominant extension/compression component and was constructed from a dataset containing 30 striae on slickensides. It was identified at the Szary Kamień site as a paleostress state SK-3 and in the Lutynia active quarry as a paleostress state LQ-1 (Fig. 4). The phase must have appeared between 4.56 ± 0.20 Ma and 3.83 ± 0.17 Ma (Early Pliocene). The orientation of the principal axes is σ1 164°/19° and σ3 67°/18°. The planes with the maximum shear stress are oriented 129°/84°to the S as a dextral/reverse fault and 7°/65° to the W as a sinistral/normal fault. The plane with the highest tendency to dilate has an orientation of 157°/72° to the W. This stress field produced the subsidence of the northern blocks against the southern ones on the E-W to NW-SE striking faults, also with a dextral sense of movement. The sinistral faults striking NE-SW were also activated (see the block diagram in Fig. 4).

4.4 Late Pliocene NNE-SSW compression - PPD

This compression phase was constructed based on a dataset containing 27 striae on slickensides. It was identified in the Čedičový vrch hill inactive quarry as a paleostress state CH-1 and on the Czarne Urwisko/Bazaltowe Słupy outcrop as a paleostress state CU-1. The phase must have appeared after 3.83 ± 0.17 Ma (Early Pliocene) but before the PPE (see below). The orientation of the principal axes is σ1 17°/11° and σ3 115°/33°. The planes with maximum shear stress are oriented 56°/68°to the N as a sinistral/reverse fault and 167°/56° to the W as a dextral/reverse fault. The plane with the highest tendency to dilate has an orientation of 205°/57° to the W. This stress field configuration produced the horst-like relief along the faults striking ENE-WSW and NW-SE (see the block diagram in Fig. 4).

4.5 Late Pliocene-Early Pleistocene NW-SE extension - PPE

This extension phase was constructed based on a dataset containing 28 striae on slickensides. It was identified on the Szary Kamień outcrop as a paleostress state SK-4 and in the Lutynia active quarry as a paleostress state LQ-2. The phase must have appeared after 3.83 ±

0.17 Ma (Early Pliocene), after the PPD and before the PPF (see below). The orientation of the principal axes is σ1 17°/11° and σ3 115°/33°. The planes with maximum shear stress are oriented 56°/68° to the N as a sinistral/reverse fault and 167°/56° to the W as a dextral/reverse fault. The plane with the highest tendency to dilate has an orientation of 66°/75° to the S. This stress field caused subsidence of the southern blocks against the northern ones along the faults striking NW-SE and NE-SW, both with a dextral horizontal component. In addition, the western blocks are subsiding against the eastern ones along the N-S striking faults with a sinistral horizontal sense of movement (see the block diagram in Fig. 4).

4.6 Late Pliocene-Early Pleistocene NE-SW extension - PPF

This extension phase was constructed based on a dataset containing 31 striae on slickensides. It was identified in the Čedičový vrch hill inactive quarry as a paleostress state CH-2 and on the Czarne Urwisko/Bazaltowe Słupy outcrop as a paleostress state CU-2. This phase must have appeared after 3.83 ± 0.17 Ma (Early Pliocene) and after the PPE phase. The orientation of the principal axes is σ1 319°/23° and σ3 220°/19°. The planes with maximum shear stress are oriented 103°/85° to the N as a dextral/reverse fault and 162°/62° to the E as a sinistral/normal fault. The plane with the highest tendency to dilate has an orientation of 310°/71° to the N. This stress field configuration caused subsidence of the northeastern blocks against the southwestern ones along the faults striking NW-SE with a sinistral horizontal component (see the block diagram in Fig. 4).

It can be assumed that the stress parameters and orientations of the activated faults have changed several times since the Late Miocene to Early Pleistocene.

4 Discussion

The paleostress events of the Late Miocene to Quaternary observed in the area of Lutynia/Lądek Zdrój were compared with the stress field of broader regional or sub-continental dimensions.

4.1 The character of tectonic evolution of the Alpine and North Carpathian forelands since the Middle Miocene to date

The present N to NW oriented compressional stress regime of the Alpine and North Carpathian forelands reflects a combination of forces related to the continued counterclockwise convergence of the Africa-Arabia plates with Europe, and consequently collisional interaction of the Alpine orogen with its foreland, and the North Atlantic ridge push. The interplay of stress impulses generated by both the above- mentioned sources has created the paleostress/tectonic history of the European Alpine foreland (EAF) at least during the Pliocene and Quaternary (Müller et al., 1992; Dèzes et al., 2004; Ziegler & Dèzes, 2007). The switching of compressional and extensional pulses derived from both sources has caused the movement of large crustal blocks or whole regions in the Alpine foreland. The periods of uplift followed by erosion switched with periods of dominant subsidence followed by sediment deposition. In addition, the

periods of increased frequency of volcanic events indicate the lower intensity of compression (cf. Fossen, 2010).

The European Alpine foreland can be divided into three zones. The first zone represents the narrow stripe-shape zone in front of the Alps, which matches more-or-less with the North Alpine Molasse basin (Fig. 5). This zone coincides with the rapid elevation of the Alps since the Middle Miocene (Rasser & Harzhauser, 2008). The second zone comprises the southern part of the western- and middle-EAF, which coincides with the zone of Variscan crystalline European massifs (Fig. 5). This zone is characterized as sub-continually uplifting crystalline massifs, which are separated by simultaneous episodical subsidence of the European Cenozoic Rift System (ECRIS; Dèzes et al, 2004; Ziegler & Dèzes, 2007, Fig. 5). The Bohemian Massif, including the study area, is situated within this zone. The third zone is represented by the northern/outer part of the EAF marked by the North Sea-North German basin and Polish Lowlands basins (Fig. 5). The continuous subsidence in this zone has been active since the Miocene (Ziegler & Dèzes, 2007).

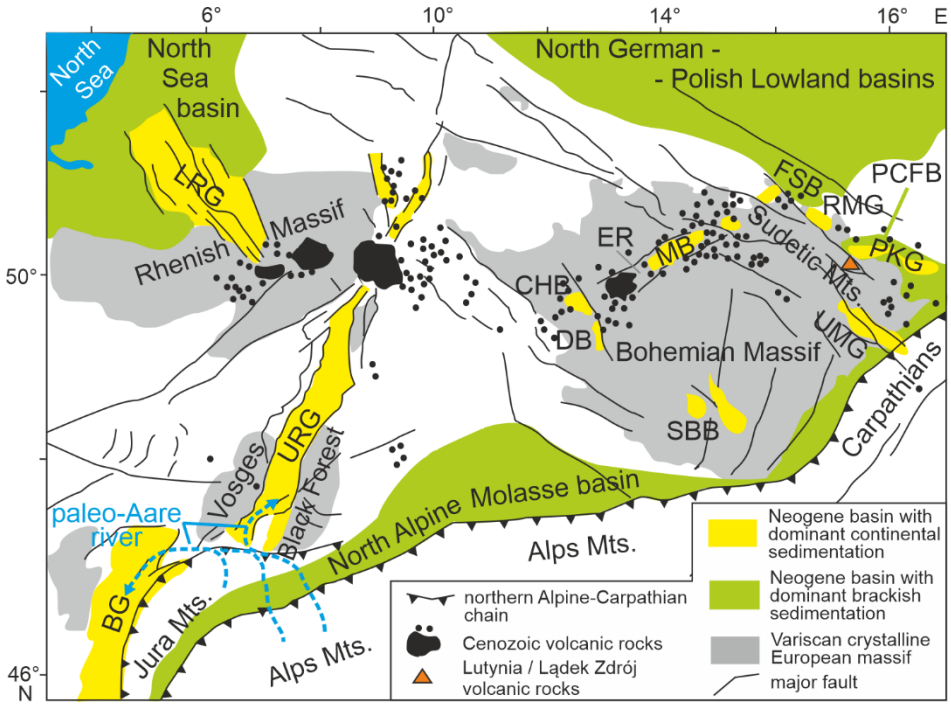

Figure 5. The schematic map of the main Cenozoic tectonic features in the European Alpine foreland (modified after Dèzes et al., 2004; Dyjor, 1981; Sissingh, 2006). FSB – Fore-Sudetic block; PCFB – Polish Carpathian Foredeep basin; the Neogene basins: BG – Bresse graben, CHB – Cheb basin, DB – Domažlice basin, ER – Eger rift, LRG – Lower Rhine graben, MB –

Most basin, PKG – Paczków – Kędzierzyn graben, RMG – Roztoki – Mokrzeszowa graben, SBB – South Bohemian basins, UMG – Upper Morava graben, URG – Upper Rhine graben.

Fig. 6 includes a comparison of the main tectonic events within the western and northern European Alpine foreland (WNEAF) with paleostress patterns in the Bohemian massif and the ones derived in the Lutynia/Lądek Zdrój area since the Middle Miocene to Pleistocene.

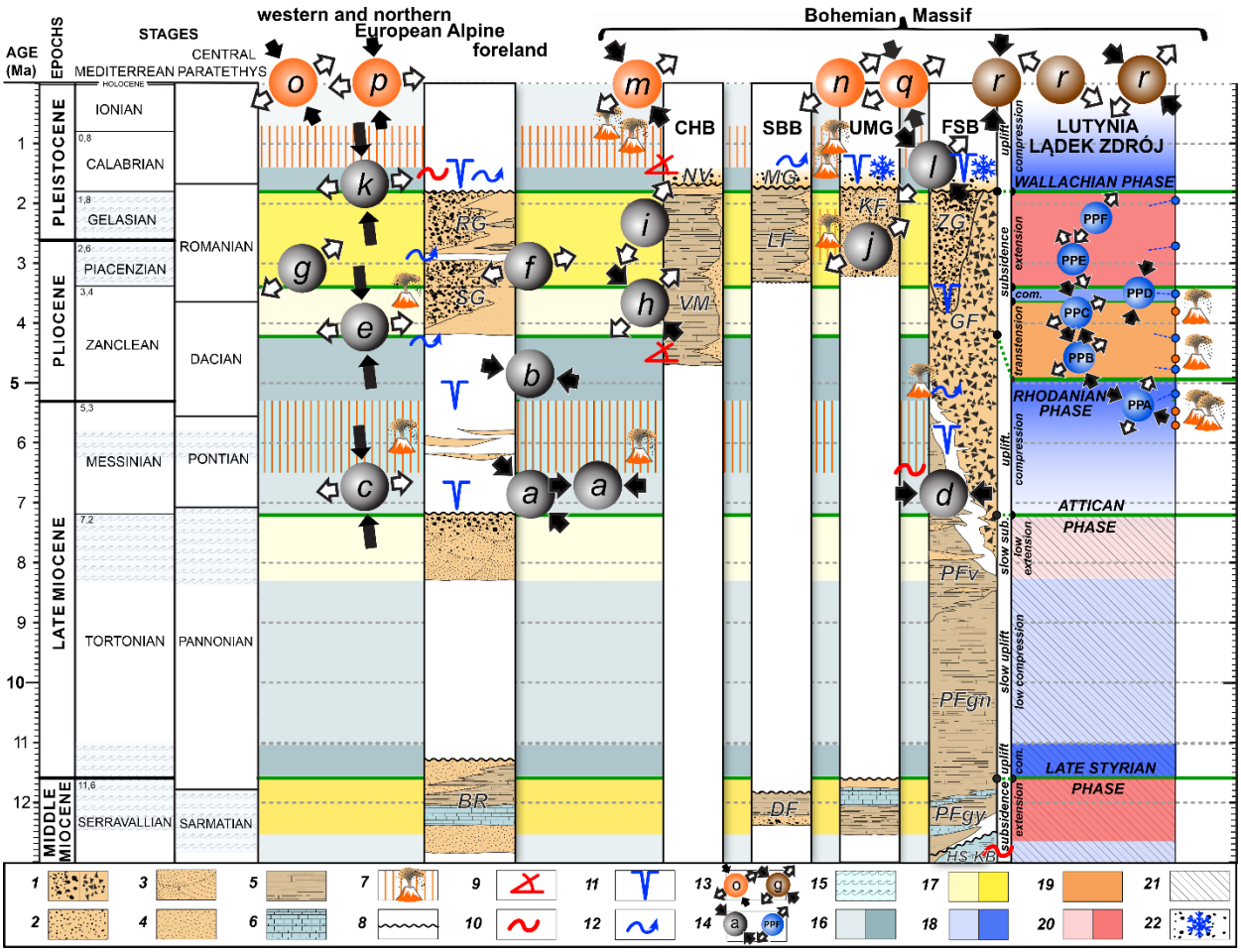

Figure 6. The comparison of the tectonostratigraphic evolution, the volcanic activity and the paleostress events within the Western and Northern European Alpine foreland (WNEAF) and the Bohemian Massif observed by other authors (the comprehensive symbols of the stress marked as a, b, …) with the paleostress events observed within the Lutynia / Lądek Zdrój area (the comprehensive symbols of the stress marked as PPA-PPF) since Middle Miocene to-date. The compared areas: WNEAF – with emphasis on the evolution in the Upper Rhine Graben and the Jura Mts.; the Bohemian Massif – with emphasis on the evolution in the CHB – Cheb Basin, SBB – South Bohemian basins, UMG – Upper Moravia graben and FSB – Fore-Sudetic block. 1 – gravels, sedimentary breccia; 2 – alluvial mostly clastic sediments; 3 – fluvial sands; 4 – lacustrine mostly sandy deposits; 5 – terrestrial shales; 6 – marine and brackish sediments (mostly shales); 7 – volcanic event; 8 – erosional boundary (hiatus); 9 – angular unconformity; 10 – folding; 11 – deep erosion; 12 – river reconfiguration; 13 – comprehensive symbols of the present-day stress, for explanation and reference see chapter 5 based on letters; 14 –

comprehensive symbols of the paleostress, for the explanation and the references see chapter 4 based on letters; 15 – period with dominant sedimentation and frequent marine ingressions within the WNEAF; The tectonic regimes deduced from the tectonostratigraphic evolution and the paleostress analysis: 16 – slow / fast uplift; 17 – slow / fast subsidence; The stress states deduced: 18 – low / intensive compression, 19 – transtension (strike-slip regime); 20 – extension, low or intensive.; 21 – Tectonic regimes deduced from tectonostratigraphic evolution only; 22 – glacial or glacifluvial deposits. The sedimentary formations (for the explanation and the references see chapter 4): BR – Bois de Raube formation, DF – Domanín formation, GF – Gozdnica formation, HS – Henryk seam; KB – Kędzierzyn and Krakoviec beds; KF – Křelov formation, LF – Ledenice formation, MG – Moldavite Gravels, NV – Nová Ves formation, PFgr – Poznań formation – green clay, PFgy – Poznań formation – grey clay, PFv – Poznań formation – variegated clay, RG – Rhine or Alpine gravels, SG – Sungau gravels, VM – Vonšov member as a part of Vildštejn formation, ZG – Ziebice group.

4.1.1 Middle-Late Miocene subsidence/extension (until 11 Ma)

During the Middle Miocene, the WNEAF, including the Bohemian Massif, was located at a low elevation and the extensional regime with subsidence and sediment accumulation was dominant here. Evidence of the subsidence was documented by lacustrine sediments (Domanín formation; DF, Fig. 6) in the Southern Bohemian basins (SBB, Fig. 5; Malkovský, 1979; Pešek, ed., 2010). The fluvio-lacustrine sediments with a marine ingression record of the Lower Badenian (15 – 16.4 Ma) are also preserved in the Upper Morava graben (UMG, Fig.5; Pešek, ed., 2010; Růžička, 2016; Špaček et al., 2015). The last marine ingression in the North Alpine Molasse basin occurred during the Late Serravallian and sedimented here as the Bois de Raube formation (ca. 11 Ma; Rasser & Harzhauser et al., 2008; BR, Fig. 6). In the Cheb basin (CHB, Fig. 5) in the northwestern Bohemian Massif, the youngest Miocene sediments (Cypris formation) are preserved from the period 21.3-17 Ma (Bucha et al., 1990). While the Miocene sedimentation in the basins of the Bohemian Massif terminated around 17 Ma, it ended in the peripheral basins around the Bohemian Massif around 13-14.8 Ma (Malkovský, 1979; Pešek, ed., 2010).

The area of the Sudetic Mts., where the Rychlebské hory Mts. are situated, underwent the uplift during that period, in contrast to the Fore-Sudetic block (FSB, Fig.5), where the continental clastic sediments were deposited under brackish or shallow marine conditions. The area of the Fore-Sudetic block, mainly in Paczków-Kędzierzyn and Roztoki-Mokrzeszowa grabens (Ondra, 1968), subsided mainly during the Serravallian (Rasser & Harzhauser et al., 2008). The Paczków-Kędzierzyn grabens (PKG, Fig. 5) were covered by the Paratethys Sea coming from the Polish Carpathian Foredeep basin (PCFB, Fig. 5), where 300 m-thick layers of clayey, silty and sandy fluvial and deltaic material with coal and lignite seams were deposited (Gabriel et al., 1982) as Kędzierzyn and Krakoviec beds (KB, Fig. 6, Dyjor & Oberc, 1983; Rasser & Harzhauser et al., 2008). In contrast, the sandy-silty sediments with lenses of brown coal, and lignite clays of the Henryk seam (HS, Fig. 6; Dyjor 1986; Dyjor & Sadowska, 1986; Piwocki & Ziembińska-Tworzydło, 1995) originating from ingression of the Northern Sea were deposited in the NW part of the Fore-Sudetic block. The marine sedimentation in the PCFB culminated around 13 Ma (Middle Serravallian; Dyjor 1981a) and terminated in the western part around 12 Ma, and in the eastern part around 11.5 Ma (Upper Serravallian) as a hiatus due to uplift of the PCFB and retreat of the Paratethys Sea to the SE (cf. Rasser & Harzhauser et al.,

2008 and others). The NW part of the Fore-Sudetic block, where the Roztoki-Mokrzeszowa grabens (RMG, Fig. 5) are situated, was affected by the Jaworska volcanic phase, which deposited the layer of basaltic tuff here (Birkenmajer et al., 1977). At the end of the Middle Miocene, the stress regime switched from extensional to compressional, probably due to the stress from the thrusting of the Outer Carpathians onto the PCFB (Badura et al., 2004; Rasser & Harzhauser et al., 2008).

4.1.2 Late Miocene slow uplift/low compression and the following subsidence/extension (ca. 11–4.2 Ma)

As mentioned above, the extensional regime changed throughout the WNEAF area at the beginning of the Tortonian (Upper Miocene), when several series of compression events occurred and caused the uplift. The strong compression event, the so-called late Styrian tectonic phase (ca. 11.6 Ma, Fig. 6), caused the sudden uplift and the related increase in erosion, and termination of marine sedimentation in the WNEAF area (Sissingh, 2006).

The late Styrian tectonic phase replaced the marine character of sedimentation by continental sediments, the so-called Poznań formation, in the PCFB and FSB. The sedimentation of the Poznań formation began in the Polish Lowlands basin in the Late Badenian (ca. 12-13 Ma; Dyjor & Sadowska, 1986; Piwocki & Ziembińska-Tworzydło, 1997), and later also in the PCFB and grabens in the FSB in the Lower Pannonian (ca. 11 Ma; Dyjor, 1981a). The lower part of the Poznań formation, the so-called Grey Clay members (PFgy, Fig. 6), contains near seashore lake sediments, which were interrupted by several marine ingressions (Kasiński et al., 2002). This fact indicates that the vertical uplift during the late Styrian tectonic phase was not intensive. The uplift continued with a lower intensity during the Tortonian, when the Green Clay members (PFGn, Fig. 6) and later Variegated Clay members (PFv, Fig. 6) of the Poznań formation were deposited. The tectonic activity, documented by sedimentation of the Poznań formation, had a varied character in different parts. The occurrence of sandy-gravel alluvial fans within the Poznań formation along the southeastern margin of the FSB indicate the activity of the SMF and low uplift of the Sudetic Mts. (Ivan, 1966; Osijuk & Piwocki, 1972; Dyjor & Kuszell, 1977). In contrast, the maximum subsidence occurred within the FSB along the NW-SE and W-E oriented faults (Dyjor & Oberc, 1983). The sedimentation of the Poznań formation terminated around 8 Ma, whereas in some parts, e.g. within the PCFB, it terminated as late as in the Early Pliocene (Dyjor, 1981a).

The reactivation of faults due to NE-SW oriented compression since 11 Ma have also been documented within the northern Eastern Alps Mts. (Decker et al., 1993; Peresson & Decker, 1997b). It culminated by the retreating of the subduction boundary in the outer Carpathians and by re-orientation of compression in an E-W direction after 9 Ma and prior to 5.3 Ma (Peresson & Decker, 1997a). In addition, Alexandrowski et al. (2005) described the E-W oriented compression in the Carpathians as a stress field, which disrupted the Miocene sediments at the end of the Miocene or Early Pliocene (comprehensive symbols of the paleostress marked as d in Fig. 6).

The above-mentioned tectonostratigraphic situation indicates the varied tectonic activity in different areas. The retreating of the Poznań formation basin to the N and termination of marine ingressions during the Late Miocene were probably caused by the asymmetric uplift of

the Sudetic Mts. related to tilting of the Sudetic and Fore-Sudetic blocks to the N. The uplift was probably compensated by subsidence along the faults limiting the FSB to the N from the Polish Lowlands basin. The uplift must have been slow, as inferred from the mainly pelitic, sandy or coal character of the Poznań formation. The low intensive uplift of the whole of the Sudetic Mts. and the whole of the Bohemian Massif (Malkovský, 1979) continued up to the end of the Tortonian (7.2 Ma), which resulted in the complete retreat of the Paratethys and Poznań formation basins in the Polish Lowlands basin. A hiatus in the sedimentation occurred due to highly intensive erosion (Dyjor, 1981a; Dyjor & Sadowska, 1986) and was followed by sedimentation of a 5-15 m (locally up to 40 m) thick set of rough clastic material, mainly gravels and sands, the so-called Gozdnica formation (GF, Fig. 6; Sawicki, 1997; Badura et al., 2003). The clastic material came from the uplifting of the Sudetic Mts. and the Outer Carpathians. As the GF deposited in the FSB also contains mudflow insets, the distinctly elevated Sudetic Mts. could be inferred (Ivan, 1966; 1990).

The intensity of the ongoing uplift in the WNEAF increased during the Messinian (Late Miocene, postdate 7.2 Ma) as the so-called Attican tectonic phase and mainly during the Zanclean (Lower Pliocene, postdating 5.3 Ma) as the so-called Rhodanian tectonic phase (Meulenkamp et al., 2000a, b; Sissingh, 2006). The main event within the WNEAF during this period was the Jura folding, which is characterized as a westward-oriented thrusting of the Jura Mts. over the eastern margin of the southernmost parts of the Rhine and Bresse grabens (Fig. 5) by 3.5 km and as a general re-emplacement of the Northern Subalpine chains. The Jura folding event was induced by an E-W to NW-SE compression within the area near the Northern Subalpine chain (Bergerat, 1987 – a, Fig. 6; Blès & Gros, 1991 – b, Fig. 6; Ziegler & Dèzes, 2007) and a WNW-ESE compression in more distant areas (Ustaszewski & Schmid, 2006 – c, Fig. 6). In addition, the intensive uplift of the Sudetic Mts. resulted from the Rhodanian tectonic phase during the whole of the Lower Pliocene (Zanclean). Deposition of the GF continued on the Fore-Sudetic block (Oberc & Dyjor, 1969) and contained a thick accumulation of alluvial fans derived from the uplifting Sudetic Mts.

The Mio-Pliocene ~E-W compressional stress field described above perfectly matches the documented paleostress pattern PPA in orientation and timing (the Rhodanian tectonic phase). Moreover, the action of this stress field terminated after 5.46 Ma and prior to 4.56 Ma (Fig. 3). The faults striking W-E, which limit the basins (e.g. Paczków graben, Kędzierzyn graben), were activated during this time (Dyjor, 1981a), which agrees with the strike of the faults that have been recognized as potentially activated by the PPA stress field orientation. The SMF and parallel faults behaved as sinistral faults and may have been activated in the area around the town of Złoty Stok (Fig. 7). The Bílá Voda fault (BVF, Fig. 7) may have been activated as a dextral fault. In the zone of the Biala fault (BF), the fault dilation was dominant, with a small minority of the segments possibly being activated as sinistral strike slip faults. The faults in the central part of the RH Mts., where the volcanism occurred, may have also been activated as sinistral strike slip faults, but a vertical component must have also been present during the uplift of the RH Mts. According to the kinematic indicators in the volcanic rocks, the eastern blocks may have subsided against the western ones along the N-S striking faults. The presence of volcanism within the study area (Birkenmajer et al., 2002; Cajz et al., 2012) and other parts of the Bohemian Massif (Ulrych et al., 2013; Cajz et al., 2009) may indicate an episodical

562 relaxation of the stress around 5-5.5 Ma, which agrees with the episode of volcanism (Merle &
563 Michon, 2001) and sedimentation (Sissingh, 2001) within the WNEAF.

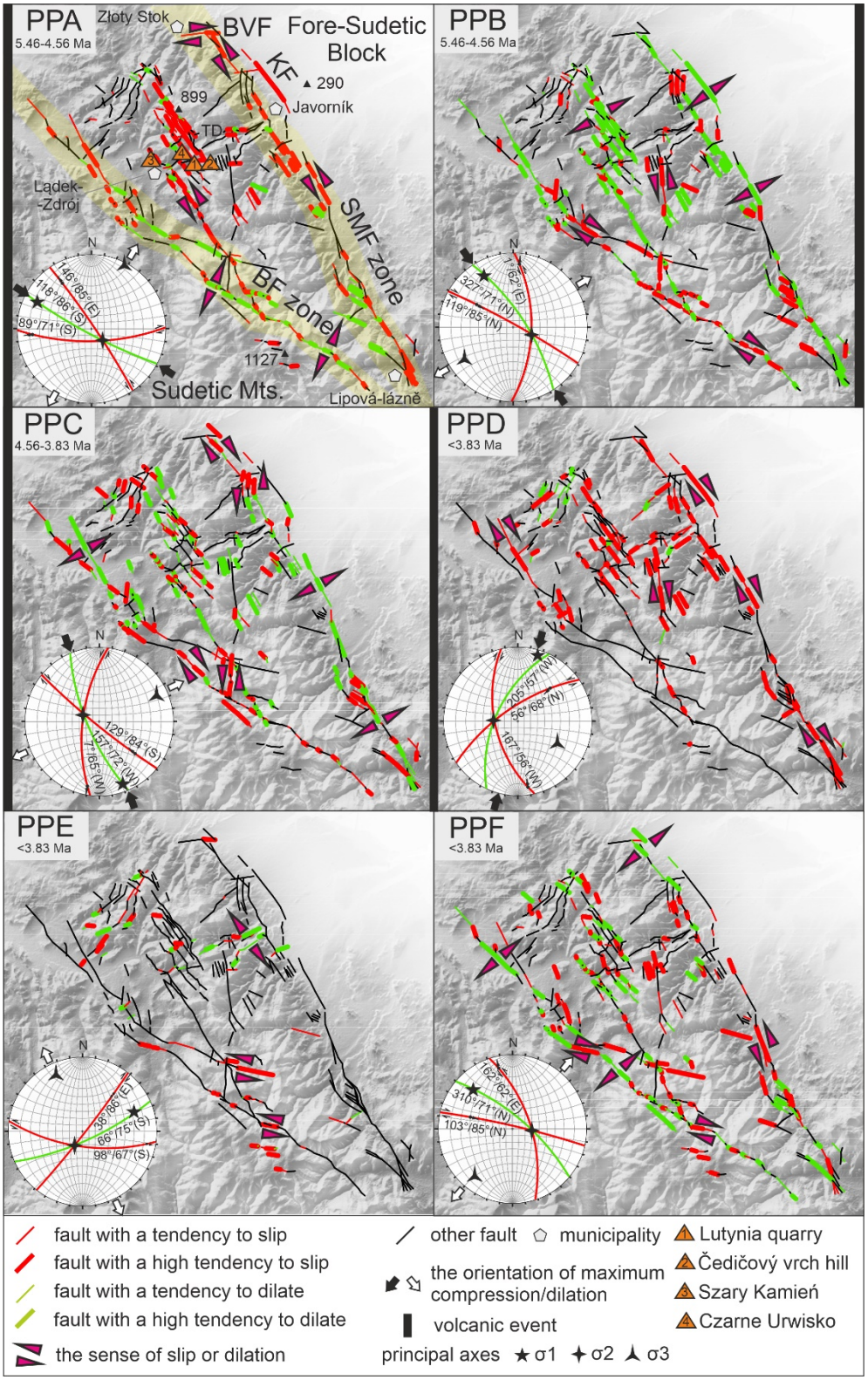

564

Figure 7. The potentially reactivated faults within the study area during action of the individual paleostress patterns in time sequence. The main faults and the fault zones: BF zone – Biala fault zone, BVF – Bílá Voda fault, KF – Kameničká fault, SMF zone – Sudetic Marginal fault zone. TD – Travná intra-mountain depression.

The very intensive uplift and compression were disrupted within the WNEAF around 4.2 Ma and this interruption is marked by undisturbed sedimentation of Sundgau gravels (SG, Fig. 6; Bergerat 1987; Blès & Gros, 1991; Ziegler, 1992; Meulenkamp et al., 2000a; 2000b; Dèzes et al., 2004; Sissingh, 2006).

4.1.3 The Pliocene-Early Quaternary subsidence/transtension and extension (4.2 – 2 Ma)

At the start of this period, distinct changes in the drainage network due to tectonic movements and opening of rift valleys occurred within the WNEAF, while fading out of the Jura folding occurred until 3.4 Ma (Giamboni et. al., 2004). For example, around 4.2 Ma, the paleo-Aare river was deflected from the Rhine Graben to the Bresse Graben (Fig. 5), where a new set of fluvial Sundgau gravels was deposited (Dèzes et al., 2004). The paleostress regime changed from reverse faulting to a strike-slip regime. The predominantly NNW-SSE oriented compression (Ustaszewski & Schmid, 2006) caused an opening of the ENE-WSW oriented ruptures (e, Fig. 6). During the Late Pliocene, the phase of rifting was renewed in the WNEAF, mainly in the Rhine graben and basins in the Western Alpine foreland. The sedimentation became confined to the accumulation of fluvio-lacustrine complexes with swamps, clastic sequences, as well as lignite-bearing marls in isolated basins (Meulenkamp et al., 2000b; Sissingh, 2006). Simultaneously with the rift subsidence, the uplift of the Variscan Massifs continued and accelerated from the Late Miocene to the Early Pliocene and during the Late Pliocene to the Quaternary (Dèzes et al., 2004; Ziegler & Dèzes, 2007). The predominantly extensional regime began around 3.4 Ma with a maximum intensity between 3 Ma and 2.5 Ma. Up to 2.9 Ma, fluvial Sundgau gravels (SG, Fig. 6) were depositing in the Bresse graben by the paleo-Aare river, which was then deflected back to the Rhine graben (Fig. 5; Giamboni et. al., 2004). Sedimentation of the Sundgau gravels terminated and a new 200 m-thick formation of Rhine gravels (RG, Fig. 6) was deposited prior to 2.0 Ma (Dèzes et al., 2004), when the extensional paleostress regime changed throughout the WNEAF (Sissingh, 2003). This provides evidence of extensional subsidence and renewed rifting in the Upper and Lower Rhine grabens, when these grabens were orthogonally extended in a NW-SE direction (Ziegler, 1992; Dèzes et al., 2004; Ziegler & Dèzes, 2007). The dominance of the extension is also documented by syn-sedimentary extensional faults and locally by positive flower-structures within the grabens in the WNEAF. All of these structures resulted from an E-W to NE-SW extension (Blès & Gros, 1991 – f, Fig. 6; Dèzes et al., 2004). Ustaszewski and Schmidt (2007) interpreted these deformations as being caused by NW-SE to N-S oriented compression (g, Fig. 6).

The same orientation of the transtensional stress field, ~NW-SE compression and ~NE-SW extension, was observed within the study area as the paleostress patterns PPB and PPC in the period between 4.56 and 3.83 Ma. Both paleostress patterns probably represent one paleostress event with transtensional parameters changing over time due to the similar orientation of the $\sigma 3$ axis. The NE-SW extension resulted in enlarging of the FSB and the Intra-Sudetic basins (e.g. Upper Nysa Kłodzka graben, UNKG, Fig. 1). The WNW-ESE to NW-SE striking faults were activated with a 70 m vertical throw and created the eastern shoulder of the UNKG (Badura &

Rauch, 2014). The WNW-ESE to NW-SE faults may have also been activated as dextral (during the PPB and PPC) and the N-S faults may have been activated as sinistral (during the PPB and PPC). The SMF zone may have tended to dilate, with only some N-S oriented segments near the town of Javorník having been activated as sinistral strike slip faults (Fig. 7). The straight trace of the SMF may have been disrupted and split by ~N-S striking faults into zigzagging segments. According to kinematic indicators in the volcanic rocks, the northern blocks mainly subsided (during the PPB and PPC) against the southern ones along the ENE-WSW to WNW-ESE striking subvertical faults (see the block diagrams in Fig. 4). These movements are reflected in the vertical contrast between the Sudetic Mts. and the Fore-Sudetic block. The BF zone may have been more active in this period. Most of the segments may have been activated as dextral strike slip faults with the expected vertical component in the range of tens of meters. The faults in the central part of the RH Mts. may have dilated, which may have corresponded to relaxation after the previous mountain ridge uplift. This transtension regime was probably terminated after the higher volcanic activity in the area of the RH Mts. and elsewhere within the Bohemian Massif (e.g. Adamovič & Coubal, 1999; Ulrych et al., 2013; Merle & Michon, 2001) around 3.83 Ma.

The Bohemian Massif underwent stagnation of the uplift or even weak subsidence during the Late Pliocene to Early Pleistocene, which is evident by the accumulation of lacustrine sediments mainly in the Cheb basin (CHB), Southern Bohemian basins (SBB) and Upper Morava graben (UMG). In the CHB, the lacustrine pelitic Vonšov member (VM, Fig. 6) as a part of the Vildštejn formation aged 4.7 Ma – 1.4 Ma (after Bucha et al., 1990; Upper Pliocene to Quaternary age after Pešek, ed., 2010) was discordantly deposited on the Cypris formation after a 12 Ma-long hiatus. The sedimentation in the Cheb and Domažlice basins (DB, Fig. 5) was caused by relative subsidence of the western block along the NNW-SSE oriented Mariánské lázně fault under a NE-SW oriented extensional regime (h, Fig. 6; Špičáková et al., 2000). In the nearby Most basin (MB, Fig. 5), the Pliocene Vysočany river terrace was faulted probably due to an NNE-SSW oriented extension (Coubal & Adamovič, 2000 – i, Fig. 6). Similarly, lacustrine sediments of the Ledenice formation (LF, Fig. 6) were deposited in the SBB and in the UMG, the Upper Pliocene to Quaternary fluvial sediments known as the Křelov formation (KF, Fig. 6) occur. The reactivation and subsidence along the NNW-SSE oriented faults caused by the ENE-WSW oriented extension are mentioned in the UMG in Růžička (2014; j, Fig. 6). Sedimentation of the Gozdnica formation continued within the area of the FSB (Dyjor, 1981a). The fluvial gravels with a kaolinic matrix, deposited in deep channels eroded in the upper part of the GF, the so-called pre-glacial formation, white gravels or the Ziebice group (ZG, Fig. 6; e.g. Przybylski et al., 1998; Dyjor, 1966; Czerwonka & Kryszkowski, 2001), have been described as being a result of Late Pliocene erosion (Walczak, 1954; 1970). The increase in bedrock erosion and common saprolite redeposition was probably caused by an increase in tectonic activity (Czerwonka & Kryszkowski, 2001) and is related also to progressive cooling of the climate (Badura et al., 2004) during the Late Pliocene and Early Pleistocene. The ZF was derived from the Sudetic Mts. being uplifted and is related to a higher erosion rate in the area of the FSB during the Middle Zanclean and Early Gelasian (Czerwonka & Kryszkowski, 2001). According to Badura et al. (2003), the pre-glacial formation originated as Pliocene gravels redeposited by sub-glacial rivers of a Mezo-Pleistocene age. In comparison to other areas of the WNEAF, the character of the ZG sediments

is similar to the character of the Sangau and Rhine gravels within the URG, where the origin of the sediments is clearly tectonic.

The above- mentioned short period of uplift during the Late Zanclean may correspond to the newly discovered event of the NNE-SSW compression described in this paper, which is represented by paleostress pattern PPD and which interrupted the period of extensional tectonic regime that lasted since the Early Pliocene. This phase is characterized as a NE-SW dominant compression. The SMF may have behaved as a dextral fault with a vertical normal component, mainly between Javorník and Złoty Stok. The BF was probably not active during this tectonic phase. The faults in the central part of the RH Mts. may have been activated as dextral faults with a vertical component (Fig. 7). According to the kinematic records in volcanic rocks, this stress regime produced the horst-like structures along the NNW-SSE and NE-SW faults (see the block diagram in Fig. 4). The subsidence of the northern and southern blocks was also suggested by Skácel and Vosyka (1959). This compressional event may have represented the stress transmission from the Carpathians as described in Stemberk Jr. et al. (2019).

The newly discovered paleostress pattern PPE is characterized as a distinct NNW-SSE oriented extension with a near normal fault regime. This hitherto unknown paleostress pattern indicates a different orientation of extension during the Piacenzian than other authors mentioned. Paleostress pattern PPE may not have affected some of the faults in the study area. No segments of the SMF zone were probably activated, only several ~W-E segments of the BF may have been activated as sinistral faults. The ENE-WSW faults, which limit the Travná intra-mountain depression (Ivan, 1966 and Stemberk Jr. et al., 2019; TD in Fig. 7) may have been dilated and created or at least morphologically accentuated this depression. The Travná depression has a complicated block-like structure in the longitudinal as well as cross-sectional profile, which agrees with the kinematic pattern derived from the data on volcanic rocks (see the block diagram of PPE in Fig. 4).

The above-mentioned ENE-WSW to NE-SW oriented extensional regime may have caused similar tectonostratigraphic evolution and deformations within the whole WNEAF and Bohemian Massif. Paleostress pattern PPF agrees with the above-mentioned extensional regime during this period. Parameters of the paleostress tensor indicate the distinct extension with a near-normal fault regime (Tab. 1) within the study area. The action of paleostress pattern PPF postdates 3.83 Ma. Paleostress pattern PPF may have affected mainly the NNW-SSE oriented faults by a sinistral sense of slip and WNW-ESE striking faults by a dextral sense of slip. The BF zone may have tended to dilate, only several short segments may have been activated as dextral faults. Within the SMF zone, several segments striking NNW-SSE may have been activated as sinistral. The straight line of the SMF may have been disrupted by the NE-SW oriented faults into zigzagging segments, which are recognizable in the relief until today. The block diagram of PPF in Fig. 4 shows the subsidence of the northeastern blocks. During this stress pattern, the northern mountain front of the RH Mts. may have been accentuated due to movement on the SMF.

4.1.4 Quaternary compressional events and uplift of massifs (ca. 2 Ma – to-date)

The regional hiatus is documented at the end of the Gelasian (about 1.8 - 2 Ma) and is related to renewed regional uplift, termination of sedimentation in the WNEAF and Bohemian

Massif, and to rapid reconfiguration of paleohydrography throughout the WNEAF (Sissingh, 2003). This distinct tectonic event corresponds to build-up of the present-day NW-SE oriented compressional stress field and is the so-called Wallachian tectonic phase. The Pliocene Sundgau gravels along the Jura Mts. front were probably folded by the same or a similar compressional impulse, postdating 2.9 Ma (Giamboni et. al., 2004). The results of the paleostress analyses indicate the N-S to NW-SE oriented compression (Ustaszewski & Schmid, 2006 – k, Fig. 6). The tectonic event that affected the whole of the Alpine and Carpathian forelands during this period is called the Wallachian phase (Hippolyte & Sandulescu, 1996).

Within the Bohemian Massif, the lacustrine sedimentation of the Gelasian (Lower Pleistocene) and Calabrian (Middle Pleistocene) sediments was replaced by locally discordantly accumulated chaotic fluvial sediments and enhanced erosion during the Early Quaternary as a response to the uplift (Malkovský, 1979). In the CHB, the sedimentation of the lacustrine Vonšov Member was replaced by heterogenous sandy gravels of the Nová Ves formation (NV, Fig. 6; Pešek, ed., 2010). In the SBB, the sedimentation of the lacustrine Ledenice formation was replaced by sandy gravels of the Moldavite Gravels (MG, Fig. 6). The uplift of the Šumava Mts. and Český les Mts. caused the deflection of the originally southward-flowing rivers to the north (Pešek, ed., 2010). In the UMG, the down-cutting erosion affected the Křelov formation, probably as a result of the Bohemian Massif uplift (Růžička, 2014). In the area of the FSB, an interruption of the sedimentation (hiatus) occurred at the beginning of the Early Pleistocene (Czerwonka & Krzyszkowski, 2001). The Sudetic Mts. were uplifted by about 60-300 m in different parts and also the FSB was uplifted by about 40-80 m (Przybylski et al., 1998) due to stress field changes and caused the reconfiguration of the drainage network and an increase in erosion (Ivan, 1966).

This stress pattern during the last period is an NW-SE oriented compression (l, Fig. 6), which was previously documented by Adamovič and Coubal (1999), Coubal et al. (2015; marked as paleostress pattern δ). The action of this stress field, which caused the uplift of the WNEAF and Bohemian Massif, was probably interrupted by several episodes of stress relaxation. This interruption is supported by young volcanism between 1.0 and 1.8 Ma (Cajz et al., 2012; Ulrych et al., 2013). Despite the stress relaxation, the continuation of episodical uplift is documented by the start of deep erosion and river terrace development around 0.7-0.8 Ma in the Variscan massifs (Ziegler & Dèzes, 2007). Moreover, the stress field has been influenced and modified by loading of the continental ice-sheet, which covered the FSB. The Middle and Late Pleistocene tectonic activity of the SMF, which was enhanced by post-glacial rebound, was suggested by faulted river terraces in the Sudetic Mts., showing 5-20 m vertical offsets in their longitudinal profiles (Krzyszkowski & Pijet 1993). The affected fluvial terraces in the FSB showed diminishing uplift intensity from the Middle Pleistocene to the Late Pleistocene based on decreasing vertical offsets of the terraces from ~20 to 3 m (Štěpančíková et al., 2008). Similar values of post-glacial uplift (post-Saalian/post-130 ka in the study area) of 20-35 m, with decreasing tendency (2-5 m in the Late Pleistocene), are reported also from the Sudetic Mts. (Badura et al., 2004), while the estimate of their total uplift along the SMF during the Middle and Late Pleistocene is 20-30 m up to 60-80 m (Krzyszkowski & Pijet 1993; Dyjor, 1981b; Przybylski, 1998; Badura & Przybylski, 1998). The decrease in the uplift intensity may have been ascribed to ice-sheet loading. Late Pleistocene activity of the SMF was also directly documented in paleoseismological trenches excavated between Złoty Stok and Javorník. The alluvial fan apex at one of the sites is truncated by the SMF and has a left-laterally offset of 30-

738 45 m from the feeder channel as a response to ice-sheet loading during the Last Glacial
739 Maximum (~20ka; Štěpančíková & Stemberk Jr., 2016).

740 Based on the World Stress Map (Heidbach et al., 2016), two distinct provinces of the
741 present-day stress field were delimited nearby the study area. The first province is the Western
742 European Stress Domain comprising the W and NW parts of the Central European Platform,
743 including the Bohemian Massif. The domain is influenced by sub-horizontal stress of NW to
744 NNW orientation caused by the push resulting from the North Atlantic Ridge spreading (Müller
745 et al., 1992; Jarosiński et al., 2006). The stress with dominant compression was determined in the
746 western part of the Bohemian Massif by Peška (1992; m, Fig. 6) based on borehole breakouts, by
747 Vavryčuk et al. (2012) based on earthquake focal mechanisms and in the eastern part by Havíř
748 (2004; q, Fig. 6) and with dominant extension by Špaček et al. (2015; n, Fig. 6) based on
749 earthquake focal mechanisms. The second province is represented by the Fore-Carpathian stress
750 domain, where the NNE-SSW to N-S oriented compression is present. The stress field is
751 generated by the tectonic push of the African plate transmitted into the foreland by ALCAPA
752 microplate. The different stress orientations in the upper (p, Fig. 6) and deeper parts of the
753 Earth's crust (o, Fig. 6) separated by a décollement layer in the Jura Mts., were presented by
754 Ustaszewski and Schmidt (2006). The present-day switching of the stress pulses of both of the
755 stress field orientations was recorded by extensometers monitoring micro-displacements on the
756 faults in the RH Mts. between 2014 and 2017 (Stemberk Jr. et al., 2019 – r, Fig. 6).

757 Nevertheless, the records of the last stress patterns have not been noticed in brittle
758 tectonics of the volcanic rocks in the study area. This is probably due to the fact that the volcanic
759 rocks reached positions near the surface, where the sub-horizontal and also normal stress field
760 cannot act due to relief geometry. The Quaternary uplift and the resulting erosion later
761 completely exposed the outcrops on the surface as elevations. The volcanic rock columns have
762 been dilating and weathered, fissures have been opened or widened due to climatic causes and
763 are no longer in direct contact, which would enable the striation process.

764 **5 Conclusions**

765 A study of paleostress markers, such as striae on slickensides, in dated volcanic rocks in
766 the Rychlebské hory Mts. resulted in the differentiation of six paleostress patterns (regimes)
767 since the Late Miocene up to ca. 2 Ma. Each paleostress pattern is characterized by the
768 orientation of the principal parameters. These paleostress patterns were discussed in the light of
769 other known paleostress patterns within the surrounding regions of the Sudetic Mts., Fore-
770 Sudetic block and the European Alpine foreland. The comparison rules out the possible influence
771 of thermic changes and a possible striae origin due to the cooling down of the volcanic rocks or
772 ongoing quarry activity. Moreover, a comparison of the tectonostratigraphic relations of the
773 sedimentary basins in the WNEAF and Polish Lowlands basin discovered the relation between
774 periods with dominant subsidence, when the extension stress regime predominated, in contrast to
775 periods with dominant uplift, when the compressional stress regime predominated. This new
776 approach allows more accurate and detailed time constraints of the action of the paleostress
777 patterns. The results show switching of tectonic phases with dominant compression, transtension
778 or extension. The following paleostress patterns were identified.

- PPA with dominant WNW-ESE compression between 5.46 Ma and 4.56 Ma, which corresponds to the end of the W-E Miocene stress field.
- PPB transtensional regime with dominant NE-SW extension between 5.46. and 4.56 Ma.
- PPC transtensional regime with a NE-SW extension character between 4.56 Ma and 3.83 Ma.
- PPD with dominant NE-SW compression postdating 3.83 Ma.
- PPE with dominant NNW-SSE extension postdating 3.83 Ma
- PPF with dominant ENE-WSW extension postdating 3.83 Ma

Because the stress conditions are crucial for the evolution of the Earth's surface, the activity and expected behavior of the fault systems within the study area during the individual periods of the paleostress patterns were suggested as presented in Fig. 7. This figure indicates the episodical re-activation of several segments of the Sudetic Marginal fault and Bělský fault. The results are given in a wide context by other authors, who deal with the evolution of the Sudetic Mts., the Fore-Sudetic block and also in the whole of the European Alpine foreland.

The newly discovered paleostress pattern PPD may reveal a hitherto unknown short period of uplift during the Late Zanclean (postdating 3.83 Ma), which caused erosion of the upper part of the Gozdnica formation. Moreover, the sedimentation was restored within the Bohemian Massif basins after this short period. Paleostress pattern PPE was also discovered, which is characterized as a distinct NNW-SSE oriented extension with a near normal fault regime. This until now unknown paleostress pattern indicates a different orientation of the extension during the Piacenzian age. Other determined paleostress patterns are similar to the known stress regimes within the WNEAF and Polish Carpathian Foredeep basin, which indicate the supra-regional tectonic origin.

Acknowledgments

This research was carried out in the framework of the Charles University in Prague, Czechia, supported by project GAUK862213 - Multidisciplinary geophysical survey in investigation of landforms, and within long-term conceptual development research organization of the Czech Academy of Sciences RVO: 67985891. Some parts were conducted thanks to support of research program KONTAKT II by Ministry of Education, Youth and Sports of the Czechia as project LH12078 - Assessment of Tectonic Movements on Active faults, the project

no. LTV20022 in research program INTER-EXCELLENCE and the project CzechGeo/EPOS - Sci CZ.02.1.01/0.0/0.0/16_013/0001800.

Datasets for this research are available in this citation references: Stemberk, J. jr. (2020) with license CC BY 4.0.

References

Adamovič, J., & Coubal, M. (1999). Intrusive geometries and Cenozoic stress history of the northern part of the Bohemian Massif. *Geolines, 9*, 5-14.

Aleksandrowski, P., Kryza, R., Mazur, S., Pin, C., & Zalasiewicz, J. A. (2000). The Polish Sudetes: Caledonian or Variscan?. *Transactions of the Royal* Society, Edinburgh, 90, 127–146. http://doi.org/10.1017/S0263593300007197

Aleksandrowski, P., & Mazur, S. (2002). Collage tectonics in the northeasternmost part of the Variscan Belt: the Sudetes, Bohemian Massif. In Winchester, J., Pharaoh, T., & Verniers, J. (Eds.), Palaeozoic Amalgamation of Central Europe. *Geological Society, London, Special Publications, 201*, 237–277. http://doi.org/10.1144/GSL.SP.2002.201.01.12

Alexandrowski, P., Krzywiec, P., Ryzner-Siupik, B., Papiernik, B., Siupik, J., Mastalerz, K., et al. (2005). The Anatomy of Strike-Slip Gas-Bearing Structure of Ryszkowa Wola (Carpathian Foreland Basin, SW Poland) as Revealed by 3D Seismics: a Product of Late Sarmatian-Pliocene (?) Episode of E–W Directed Tectonic Compression. *Geolines, 19*, 16-17.

Allmendinger, R. W., Cardozo, N. C., & Fisher, D. (2012). Structural Geology Algorithms: Vectors & Tensors. *Cambridge University Press*, 289 pp. http://doi.org/10.1017/CBO9780511920202

Angelier, J. (1989). From orientation to magnitudes in paleostress determination using fault slip data. *Journal of Structure Geology, 11*, 37-50. https://doi.org/10.1016/0191-8141(89)90034-5

Angelier, J. (1994). Inversion of brittle tectonic data in order to determine stress tensor – faults, non-faults and pressure tension structures. *Bulletin de la Societe Geologique de France, 165*(3), 211-220.

Angelier J., Tarantola A., Valette, B., & Manoussis, S. (1982). Inversion of field data in fault tectonics to obtain the regional stress - 1. Single phase fault populations: a new method of computing the stress tensor. *Geophys. J. R. astr. Soc., 69*, 607-621. http://doi.org/10.1111/j.1365-246X.1982.tb02766.x

Badura, J., & Przybylski, B. (1998). Zasięgi lądolodów plejstoceńskich i deglacjacja obszaru między Sudetami a Wałem Śląskim (Extent of the Pleistocene ice sheets and deglaciation between the Sudeten and the Silesian Rampart), *Biuletyn Państwowego Instytutu Geologicznego (Journal of the Polish national geological institute), 385*, 9-27. (in Polish with English abstract)

Badura, J., Przybylski, B., & Zuchiewicz, W. (2004). Cainozoic evolution of Lower Silesia, SW Poland: A new interpretation in the light of sub-Cainozoic and sub-Quaternary topography. *Acta Geodyn. Geomater, 1* (135), 7-29.

Badura, J., Zuchiewicz, W., Górecki, A., Sroka, W., Przybylski, B., & Żyszkowska, M. (2003). Morphotectonic properties of the Sudetic Marginal Fault, SW Poland. *Acta Montana, A, 24*(131), 21-49.

Badura, J., Zuchiewicz, W., Štěpančíková, P., Przybylski, B., Kontny, B., & Cacoń, S. (2007). The Sudetic Marginal Fault: A young morphotectonic feature at the NE margin of the Bohemian Massif, Central Europe. *Acta Geodyn. Geomater., 4*(148), 7-29.

Badura, J., & Rauch, M. (2014). Tectonics of the Upper Nysa Kłodzka Graben, the Sudetes. *Geologia Sudetica, 42*, 137–148.

Berger, F. (1932). Die Alterstellung des Basaltes vom Grauer Stein bei Landeck, Grafschaft Glatz (The position of volcanics of the Szary Kamień by Lądek Zdrój, county Glatz). *Entralblatt für Min., B*, 545-553.

Bergerat, F. (1987). Stress field in the European platform at the time of Africa–Eurasia collision. *Tectonics, 6*, 99–132. http://doi.org/10.1029/TC006i002p00099

Birkenmajer, K., Jeleńska, M., Kądziałko-Hofmokl, M., & Kruczyk, J. (1977). Age of deep-seated fracture zones in Lower Silesia (Poland), based on K-Ar and paleomagnetic dating of Tertiary basalts. *Annales de la Société Géologique de Pologne, 47*(4), 545-552.

Birkenmajer, K., Pécskay, Z., Grabowski, J., Lorenc, M. W., & Zagożdżon, P. (2002). Radiometric dating of the Tertiary volcanics in Lower Silesia, Poland. II. K-Ar and paleomagnetic data from Neogene basanites near Lądek Zdrój, Sudetes Mts.. *Annales Societatis Geologorum Poloniae, 72*, 119-129.

Blès, J.-L., & Gros, Y. (1991). Stress field changes in the Rhone Valley from the Miocene to the present. *Tectonophysics, 194*, 265–277. https://doi.org/10.1016/0040-1951(91)90264-S

Bucha, V., Horáček, J., & Malkovský, M. (1990). Palaeomagnetic stratigraphy of the Tertiary of the Cheb Basin (W Bohemia). *Věstník Ústředního ústavu geologického (Journal of Geological institute), 65*(5), 267-278. (in Czech)

Buday, T., Ďurica, D., Opletal, M., & Šebesta, J. (1997). Význam bělského a klepáčovského zlomového systému a jeho pokračování do Karpat (The importance of the Bělá and Klepáčov fault system and their continuation to Carpathians). *URGP (Journal of Coal, ore and geological investigations), 9*, 275-281. (in Czech)

Cajz, V., Rapprich, V., Schnabl, P., & Pécskay, Z. (2009). Návrh litostratigrafie neovulkanitů východočeské oblasti (A proposal on lithostratigraphy of Cenozoic volcanic rocks in Eastern Bohemia). *Geoscience Research Reports for 2008*, 9-14. (in Czech)

Cajz, V., Schnabl, P., Pécskay, Z., Skácelová, Z., Venhodová, D., Šlechta, S., & Čížková, K. (2012). Chronological implications of the paleomagnetic record of the Late Cenozoic volcanic activity along the Moravia-Silesia border (NE Bohemian Massif). *Geologica Carpathica, 63*(5), 423-435. http://doi.org/10.2478/v10096-012-0033-3

Coubal, M., & Adamovič, J. (2000). Youngest tectonic activity on faults in the SW part of the Most Basin. *Geolines, 10*, 15-17.

Coubal, M., Málek, J., Adamovič, J., & Štěpančíková, P. (2015). Late Cretaceous and Cenozoic dynamics of the Bohemian Massif inferred from the paleostress history of the Lusatian Fault Belt. *Journal of Geodynamics, 87*, 26-49. http://doi.org/10.1016/j.jog.2015.02.006

Cwojdziński, S. (1977). Szczegółowa Mapa Geologiczna Sudetów, 902C-Trzebieszowice (Geological maps of Sudetes, sheet 902C-Trzebieszowice). *Institut Geologiczny (Polish Geological Institute).*

Cwojdziński, S. (1981). Szczegółowa Mapa Geologiczna Sudetów, 934A-Stronie Śląskie (Geological maps of Sudetes, sheet 934A-Stronie Śląskie). *Institut Geologiczny (Polish Geological Institute).*

Cymerman, Z., & Cwojdziński, S. (1984). Szczegółowa Mapa Geologiczna Sudetów, 934B-Strachocin, Bielice (Geological maps of Sudetes, sheet 934B-Strachocin, Bielice). *Institut Geologiczny (Polish Geological Institute).*

Czerwonka, J. A., & Krzyszkowski, D. (2001). Preglacial (Pliocene – Early Middle Pleistocene) deposits in Southwestern Poland: lithostratigraphy and reconstruction of drainage pattern. In: Krzyszkowski, D. (Ed.), Late Cainozoic Stratigraphy and Palaeogeography of the Sudetic Foreland. *Wind, J. Wojewoda*, 147-195.

Danišík, M., Štěpančíková, P., & Evans, N. J. (2012). Constraining long-term denudation and faulting history in intraplate regions by multisystem thermochronology: An example of the Sudetic Marginal Fault (Bohemian Massif, central Europe). *Tectonics, 31*. http://doi.org/10.1029/2011TC003012

Decker, K., Meschede, M., & Ring, U. (1993). Fault slip analysis along the northern margin of the Eastern Alps (Molasse, Helvetic nappes, North and South Penninic flysch, and the Northern Calcareous Alps). *Tectonophysics, 223*(3-4), 291-312. http://doi.org/10.1016/0040-1951(93)90142-7

Dèzes, P., Schmid, S. M., & Ziegler, P. A. (2004). Evolution of the European Cenozoic Rift System: interaction of the Alpine and Pyrenean orogens with their foreland lithosphere. *Tectonophysics, 389*, 1–33, http://doi.org/10.1016/j.tecto.2004.06.011

Don, J., Skácel, J., & Gotowała, R. (2003). The boundary zone of the East and West Sudetes on the 1:50 000 scale geological map of the Velké Vrbno, Staré Město and Śnieżnik Metamorphic Units. *Geologia Sudetica, 35*, 25–59.

Dyjor, S. (1981a): Ewolucja trzeciorzędowych przedgórskich rowów tektonicznych centralnych i wschodnich Sudetów (The evolution of the Tertiary tectonics in central and eastern part of the Sudetes). In Kwiecień, L. (Ed.), III. Sympozjum - Współczesne i neotektoniczne ruchy skorupy ziemskiej w Polsce (III. Symposium – Present-day and neotectonic movements of the earth's crust in Poland). *Ossolineum, Wrocław*, 155–181. (in Polish with English summary)

Dyjor, S. (1981b). Problemy wieku dolnej granicy i fazy ruchów neotektonicznych w południowo-zachodniej Polsce (The age of the lower limit and phases of the neotectonic movements in southwestern Poland). In Kwiecień, L. (Ed.), III. Sympozjum - Współczesne i neotektoniczne ruchy skorupy ziemskiej w Polsce (III. Symposium – Present-day and neotectonic movements of the earth's crust in Poland). *Ossolineum, Wrocław*, 25-41. (in Polish with English summary)

Dyjor, S. (1986). Evolution of sedimentation and paleogeography of near-frontier areas of the Silesian Part of the Paratethys and Tertiary Polish-German Basin. *Kwartalnik AGH, Geol., 12*(3), 7-24.

Dyjor, S. (1966). Wiek serii białych żwirów i glin kaolinowych w zachodniej części przedpola Sudetów, (The age of the white gravels and kaolinic soils in the western part of the Sudetic Foreland). *Prz. Geol., 14*, 478-479. (in Polish)

Dyjor, S., & Sadowska, A. (1986). An attempt of correlation of stratigraphic and lithostratigraphic units of Tertiary in western part of Polish Lowlands and Silesian part of Paratethys (IGCP 25). *Przegląd Geologiczny, 7*, 380–386.

Dyjor, S., & Kuszel, T. (1977). Neogeńska i czwartorzędowa ewolucja rowu tektonicznego Roztoki-Mokrzeszowa (Neogene and Quaternary evolution of the Roztoki-Mokrzeszow tectonic grabens). *Geologia Sudetica, 13*(3).

Dyjor, S., & Oberc, J. (1983). Recent crustal movements in SW Poland causing possible damage in mines and in idustrial objects, Materiały III Krajowego Sympozjum "Współczesne i neotektoniczne ruchy skorupy ziemskiej w Polsce". *Ossolineum, Wrocław, 4*, 7-23. (in Polish, with English summary)

Farr, T. G., (Eds.) (2007). The Shuttle Radar Topography Mission. *Rev. Geophys., 45, RG2004*, Last access: 12 Nov 2018. https://www2.jpl.nasa.gov/srtm, http://doi.rg/10.1029/2005RG000183

Fediuk, F., & Fediuková, E. (1989). Ultramafická nodule severomoravských bazaltoidů (Ultramafic nodules in basalts from northern Moravia, Czechoslovakia). *Sbor. Geol. Věd – Geologie (Journal of Geological Sciences – Geology), 44*, 9-49.

Fossen, H. (2010). Structure Geology. *Cambridge University Press, New York*, 463 pp. http://doi.org/10.1017/CBO9780511777806

Franke, W., & Żelaźniewicz, A. (2000). The eastern termination of the Variscides: terrane correlation and kinematic evolution. In Franke, W., Haak, V., Oncken, O., & Tanner, D. (Eds.), Orogenic Processes: Quantification and Modelling in the Variscan Belt. *Geological Society, London, Special Publications, 179*, 63–86. http://doi.org/10.1144/GSL.SP.2000.179.01.06

Gabriel, M., Gabrielová, N., Hokr, Z., Knobloch, E., & Kvaček, Z. (1982). Miocén ve vrtu Vidnava Z-1 (Miocene formation in borehole by Vidnava town). *Journal of Geological Sciences, part Geology, 36*, 115-137. (in Czech)

Giamboni, M., Ustaszewski, K., Schmid, S. M., Schumacher, M. E., & Wetzel, A. (2004). Plio-Pleistocene transpressional reactivation of Paleozoic and Paleogene structures in the Rhine-Bresse transform zone (northern Switzerland and eastern France). *Int J Earth Sci (Geol. Rundsch), 93*, 207–223. http://doi.org/10.1007/s00531-003-0375-2

Gierwielanic, J. (1968). Szczegółowa Mapa Geologiczna Sudetów, 902D-Lądek Zdrój (Geological maps of Sudetes, sheet 902D-Lądek Zdrój). *Institut Geologiczny (Polish Geological Institute)*.

Guterch, B., & Lewandowska-Marciniak, H. (2002). Seismicity and seismic hazard in Poland. *Folia Quaternaria, 73*, 85-99.

Havíř, J. (2002). Variscan and Post-Variscan Paleostresses on the Southeastern Margin of the Nízký Jeseník Region (Czech Republic). *Geolines, 14*, 33-34.

Havíř, J. (2004). Orientation of recent principal stress axes in the Jeseníky region. *Acta Geodyn. Geomater., 1*(135), 49-57.

Heidbach, O., Rajabi, M., Reiter, K., Ziegler, M., & WSM Team (2016). World Stress Map Database Release 2016. *GFZ Data Services*. http://doi.org/10.5880/WSM.2016.001

Hippolyte, J. C., Bellier, O., & Espurt, N. (2012). Quaternary deformation and stress perturbations along the Digne thrust front, Southwestern Alps. *Comptes Redus Geoscience, 344*(3-4), 205-213. http://doi.org/10.1016/j.crte.2012.03.002

Hippolyte, J. C., & Sandulescu, M. (1996). Paleostress characterization of the "Wallachian phase" in its type area (southeastern Carpathians, Romania). *Tectonophysics, 263*(1-4), 235-248. http://doi.org/10.1016/S0040-1951(96)00041-8

Hynie, O. (1963). Minerální vody (Mineral waters). *Nakl. Československ. Akad. Věd (Czechoslovak Academy of Sciences press)*, 797 pp. (in Czech)

Ivan, A. (1990). K charakteru neotektonických pohybů a vývoji reliefu v oblasti Hrubého Jeseníku a východní části Orlických hor (The character of the neotectonic movements and relief evolution in Hrubý Jeseník Mts. and eastern part of the Orlické hory Mts.). *Čas. Slez. Muz. (Journal of the Silesian Museum), A, 39*, 277-281.

Ivan, A. (1966). Geomorfologické poměry severozápadní části Rychlebských hor, Kandidátská práce (Geomorphological conditions of NW part of the Rychlebské hory Mts., Ph.D. theses). *Geological Institute of the Czechoslovak Academy of Sciences, Brno*, 120 pp. (in Czech)

Ivan, A. (1997). Topography of the Marginal Sudetic Fault in the Rychlebské hory Mts. and geomorphological aspects of epiplatform orogenesis in the NE part of Bohemian Massif. *Moravian Geographic Reports, 5*, 3-17.

Jarosiński, M., Beekman, F., Bada, G., & Cloetingh, S. (2006). Redistribution of recent collision push and ridge push in Central Europe: Insights from FEM modelling. *Geophys. J. Int., 167*, 860–880. http://doi.org/10.1111/j.1365-246X.2006.02979.x

Jelínek, J. (2008). Morphotectonic analysis of the digital relief model – a suitable means of searching for zones of rock mass britle failure. *GeoScience Engineering, 54*(3), 1-13.

Kasiński, J. R., Czapowski, G., & Gąsiewicz, A. (2002). Marine-influenced and continental settings of the Poznań Formation (Upper Neogene, Central and SW Poland). In Gürs, K. (Ed.), Northern European Cenozoic Stratigraphy, Proceedings of the 8th Biannual Meeting of the RPCSS/RNCSS. *Landesamt für Natur und Umwelt des Landes Schleswig-Holstein, Flintbek*, 162–184.

Kasza, L. (1964). Geology of the upper basin of the Biala Lądecka stream. *Geol. Sudet, 1*, 119-167.

Kontny, B. (2004). Is the Sudetic Marginal Fault still active? Results of the GPS monitoring 1996-2002. *Acta Geodyn. Geomater., 1*(135), 35-39.

Kroner, U., Mansy, J.-L., Mazur, S., Aleksandrowski, P., Hann, H.P., Huckriede, H., et al. (2008). Variscan tectonics. In McCann, T. (Ed.), The geology of Central Europe. *The Geological Society, London*, pp. 599–664. http://doi.org/10.1144/CEV1P.11

Krzyszkowski, D., & Pijet, E. (1993). Morphological effects of Pleistocene fault activity in the Sowie Mts., southwestern Poland. *Zeitschr. Geomorph., N. F., Suppl.-Bd. 94*, 243–259.

Krzyszkowski, D., Migoń, P., & Sroka, W. (1995). Neotectonic Quaternary history of the Sudetic Marginal fault, SW Poland. *Folia Quaternaria, 66*, 73–98.

Krzyszkowski, D., Przybylski, B., & Badura, J. (2000). The role of neotectonics and glaciation on terrace formation along the Nysa Kłodzka River in the Sudeten Mountains, southwestern Poland. *Geomorphology, 33*(3-4), 149–166. http://doi.org/10.1016/S0169-555X(99)00123-3

Málek, J., Fischer, T., & Coubal, M. (1991). Computation of regional stress tensor from small scale tectonic data, *Publ. Inst. Geophys. Pol. Acad. Sci., M-15(235)*, 77–92.

Malkovský, M. (1979). Tektogeneze platformního pokryvu Českého masívu (Tectogeny of the platform cover of the Bohemian Massif). *Knihovna ÚÚG (Library of the Geological institute), 53*, 176 pp. (in Czech)

Map portal of Czech Geological Survey. Last access: 14 Feb 2019. https://mapy.geology.cz

Marrett, R. A., & Allmendinger, R. W. (1990). Kinematic analysis of fault-slip data. *Journal of Structural Geology, 12*, 973-986. http://doi.org/10.1016/0191-8141(90)90093-E

Mazur, S., Aleksandrowski, P., Kryza, R., & Oberc-Dziedzic, T. (2006). The Variscan Orogen in Poland. *Geol. Q., 50*(1), 89–118.

Merle, O., & Michon, L. (2001). The formation of the West European rift. A new model as exemplified by the Massif Central area. *Societé Géologique de France, 172*, 213-221. http://doi.org/10.2113/172.2.213

Meulenkamp, J. E., Sissingh, W., Calvo, J. P., Daams, R., Londeix, L., Cahuzac, B., et al. (2000a). Late Tortonian (8.4-7.2 Ma). In Dercourt J., Gaetani M., Vrielynck B., Barrier E., Biju-Duval B., Brunet F. M., et al. (Eds.): Peri-Tethys Atlas, Palaeogeographic Maps with Explanatory Notes. *CCGM/CGMW, Paris*, 195-201.

Meulenkamp, J. E., Sissingh, W., Calvo, J. P., Daams, R., Londeix, L., Cahuzac, B., et al. (2000b). Piacenzian / Gelasian (3.4-1.8 Ma). In Dercourt, J., Gaetani, M., Vrielynck, B., Barrier, E., Biju-Duval, B., Brunet, F. M., et al. (Eds.): Peri-Tethys Atlas, Palaeogeographic Maps with Explanatory Notes. *CCGM/CGMW, Paris*, 203-208.

Morris, A., Ferrill, D. A., & Henderson, D.B. (1996). Slip tendency analysis and fault reactivation. *Geology 24*(3), 275-278. http://doi.org/10.1130/0091-7613(1996)024<0275:STAAFR>2.3.CO;2

Müller, B., Zoback, M. L., Fuchs, K., Mastin, L. Gregersen, S., Pavoni, et al. (1992). Regional patterns of tectonic stress in Europe. *J. geophys. Res., 97*(B8), 11783-11803. http://doi.org/10.1029/91JB01096

Müller, V., & Čurda, J. (2003). Vysvětlivky k souboru geologických a ekologických účelových map přírodních zdrojů v měřítku 1:50 000, Listy 04-43, 04-44, 14-21, 14-22, Bílý Potok, Javorník, Travná, Jeseník (Notes to geological and ecological maps of nature resources in scale 1:50 000, Sheets 04-43, 04-44, 14-21, 14-22, Bílý Potok, Javorník, Travná, Jeseník. *Czech Geological Survey*, 80 pp. (in Czech)

Nováková, L. (2010). Detail brittle tectonic analysis of the limestones in the quarries near Vápenná village (case study). *Acta Geodyn. Geomater., 7*(158), 167–174.

Oberc, J. (1972). Budowa Geologiczna Polski, Tektonika, Sudety i obszary przyległe (Geological setting of the Poland, Tectonics, Sudetes and surrounding area). *Wydawnictwa Geologiczne (Geological press), Warszawa*, 1–307. (in Polish)

Oberc, J., & Dyjor, S. (1969). Marginal Sudetic Fault. *Journal of the Geological Institute, 236*, 41-142. (in Polish with English summary)

Ondra P. (1968). Zpráva o vrtném průzkumu miocénní pánve u Uhelné ve Slezsku (Reports of the drilling campagne within the Miocene graben by Uhelná village). *Geoscience Research Reports, 1*, 266-267. (in Czech)

Osijuk, D., & Piwocki, M.: (1972). Osady spływów błotnych w utworach trzeciorzędowych okolic Ząbkowic Śląskich (Run-off muds in the Tertiary formations near Ząbkowice Śląskie town). *Buil. Inst. Geol., 266*, 110–125. (in Polish)

Pagaczewski, J. (1972). Catalogue of earthquakes in Poland in 1000–1970 years. *Mat. I Prace Inst. Geofyz., 51*, 36 pp.

Peresson, H., & Decker, K. (1997a). Far-field effects of Late Miocene subduction in the Eastern Carpathians: E–W compression and inversion of structures in the Alpine–Carpathian–Pannonian region. *Tectonics, 16*, 38–56. http://doi.org/10.1029/96TC02730

Peresson, H., & Decker, K. (1997b). The Tertiary dynamics of the Northern Eastern Alps (Austria): changing paleostresses in a collisional plate boundary. *Tectonophysics, 272*, 125–157. http://doi.org/10.1016/S0040-1951(96)00255-7

Pešek, J. (Ed.) (1992). Terciérní pánve a ložiska hnědého uhlí České republiky (Tertiary basins and deposits of brown coal in Czech Republic). *Česká geologická služba (Czech geological survey)*, 438 pp. (in Czech)

Peška, P. (1992). Stress indications in the Bohemian Massif: reinterpretation of borehole televiewer data. *Stud. Geophys. Geod., 36*(4), 307–324. http://doi.org/10.1007/BF0162548

Pešková, I., Hók, J., Štěpančíková, P., Stemberk, J., & Vojtko, R. (2010). Results of stress analysis inferred from fault slip data along the Sudetic Marginal Fault (NE part of Bohemian Massif). *Acta Geol. Slov., 2*(1), 11-16.

Piwocki, M., & Ziembińska-Tworzydło, M. (1995). Litostratygrafia i poziomy sporowo-pyłkowe neogenu na Niżu Polskim (Neogene of the Polish Lowlands-lithostratigraphy and pollen-spore zones). *Prz. Geol., 43*(1), 916–927.

Piwocki, M., & Ziembińska-Tworzydło, M. (1997). Neogene of the Polish Lowlands – lithostratigraphy and pollen-spore zones. *Geol. Quart., 41*, 21–40.

Pospíšil, L., Otava, J., & Hudečková, E. (2019). Utilization of archive geophysical data for geodynamical studies in the Sudetes: Example of Bělá fault zone (The Nízký Jeseník Mts.). Acta Geodyn. Geomater., 3(195), 281-291. https://doi.org/10.13168/AGG.2019.0024

Pouba, Z., & Mísař, Z. (1961). O vlivu příčných zlomů na geologickou stavbu Hrubého Jeseníku (About the influence of transversal faults to geological structure of the Hrubý Jeseník Mts.). *Journal for mineralogy and geology, IV*. (in Czech)

Przybylski, B., Badura, J., Czerwonka, J. A., Krzyszkowski, D., Krajewska, K., & Kuszell, T. (1998). Preglacial Nysa Kłodzka fluvial system in the Sudetic Foreland, Southwestern Poland. *Geologia Sudetica, 31*, 171–196.

Ramsay, J. G., & Huber, M. I. (1987). The Techniques of Modern Structure Geology, Volume 2: Folds and Fractures. *Academic Press, London*, 309-697. http://doi.org/ https://doi.org/10.1017/S0016756800010384

Ramsay, J. G., & Lisle, R. J. (2000). Modern Structure Geology, Volume 3: Applications of Continuum Mechanics in Structure Geology. *Academic Press, London*, 1-560, http://doi.org/10.1016/S0040-1951(01)00270-0

Rasser, M. V., & Harzhauser, M. (2008). Palaeogene and Neogene. In Mc Cann, T. (Ed.): The Geology of Central Europe - Volume 2, Mesozoic and Cenozoic. *Geological Society, London*, 1031-1139. http://doi.org/10.1144/CEV2P.5

Růžička, M. (2016). Geologie hydrogeologického rajonu 1621 Pliopleistocén Hornomoravského úvalu – sever (Geology of the hydrogeological region 1621, Pliocene – Pleistocene in the northern part of the Upper Moravia Graben). *Česká geologická služba (Czech geological survey), Geofond*, 18 pp. (in Czech)

Sawicki, L. (1997). Mapa geologiczna regionu Dolnośłaskiego z przyległymi obszarami Czech i Niemiec 1:100 000, Podstawy litostratygraficzne i kodyfikacja Wydzieleń (The geological map of the Lower Silesia with notes). *Warszawa*, 181 pp. (in Polish)

Schenk, V., Cacoń, S., Bosy, J., Kontny, B., Kottnauer, P., & Schenková, Z. (2002). The GPS Geodynamic network East Sudeten. Five annual campaigns (1997-2001), Data processing and results. *Acta Montana, A*, (124), 13-23.

Sissingh, W. (2001). Tectonostratigraphy of the West Alpine foreland: correlation of Tertiary sedimentary sequences, changes in eustatic sea-level and stress regime. *Tectonophysics, 233*, 361–400. http://doi.org/10.1016/S0040-1951(01)00020-8

Sissingh, W. (2003). Tertiary palaeogeographic and tectonostratigraphic evolution of the Rhenish Triple Junction. *Palaegeography, Palaeoclimatology, Palaeoecology, 196*, 229-263. http://doi.org/10.1016/S0031-0182(03)00320-1

Sissingh, W. (2006). Syn-kinematic palaeogeographic evolution of the West European Platform: correlation with Alpine plate collision and foreland deformation. *Neth. J. Geosci., 85*, 131–180. http://doi.org/10.1017/S0016774600077933

Skácel, J., & Vosyka, S. (1959). Přehled geologie Rychlebských hor (Geology of the Rychlebské hory Mts.). *Rychlebské hory - sborník prací o přírodních poměrech (Rychlebské hory Mts. proceedings), 30*, 9-45. (in Czech)

Skácel, J. (1963). Geologie krystalinika a rudních výskytů ve střední části Rychlebských hor (Geology of the crystalline complex and ore in central part of the Rychlebské hory Mts). *Journal of Geological Sciences, 3*, 109-139. (in Czech)

Skácel, J. (1989). Křížení okrajového zlomu lugika a nýznerovského dislokačního pásma mezi Vápennou a Javorníkem ve Slezsku. (Crossing of the Lugicum marginal fault and Nýznerov dislocation zone between Vápenná and Javorník). *Acta Univer. Palackianae Olomucensis. Facultas rerum naturalium, T. 29. Geogr.-Geol. 28*(95), 31-45. (in Czech)

Skácel, J. (2004). The Sudetic Marginal Fault between Bílá Voda and Lipová Lázně. *Acta Geodyn. Geomater., 1*(145), 31-33.

Skácelová, D. (Ed.) (1992a). Geologická mapa ČR, 1:50 000, list 04-43 Bílý Potok (Geological map of the Czechia in scale 1:50 000, sheet 04-43 Bílý Potok. *Czech Geological Institute*.

Skácelová, D. (Ed.) (1992b). Geologická mapa ČR, 1:50 000, list 14-21 Travná (Geological map of the Czechia in scale 1:50 000, sheet 14-21 Travná. *Czech Geological Institute*.

Skácelová, D. (Ed.) (1997). Geologická mapa ČR, 1:50 000, list 04-44 Javorník (Geological map of the Czechia in scale 1:50 000, sheet 04-44 Javorník. *Czech Geological Institute*.

Sperner, B., & Zweigel, P. (2010). A plea for more caution in fault–slip analysis. *Tectonophysics, 482*(1–4), 29-41. http://doi.org/10.1016/j.tecto.2009.07.019

Špičáková, L., Uličný, D., & Koudelková, G. (2000). Tectonosedimentary evolution of the Cheb Basin (NW Bohemia, Czech Republic) between Late Oligocene and Pliocene: a preliminary note. *Studia geoph. et geod., 44*(4), 556-580. http://doi.org/10.1023/A:1021819802569

Stemberk, J., Jr., Coubal, M., Stemberk, J., & Štěpančíková, P. (2019). Stress analysis of slips data recorded within the Dědičná štola Gallery in the Rychlebské hory Mts., NE part of the Bohemian Massif. *Acta Geodyn. Geomater., 16*(195), 315-330. http://doi.org/10.13168/AGG.2019.0027

Stemberk, J., Jr. (2020). Striae on slickensides within the Lutynia/Ladek Zdroj area for SW Faultkin7 and ROCK2014. *Mendeley Data*, v1. http://dx.doi.org/10.17632/p98hwk5mwn.1

Špaček, P., Sýkorová, Z., Pazdírková, J., Švancara, J., & Havíř, J. (2006). Present-day seismicity of the south-eastern Elbe Fault System (NE Bohemian Massif). *Studia Geophysica et Geodaetica, 50*(2), 233-258. http://doi.org/10.1007/s11200-006-0014-z

Špaček, P., Bábek, O., Štěpančíková, P., Švancara, J., Pazdírková, J., & Sedláček, J. (2015). The Nysa-Morava Zone: an active tectonic domain with Late Cenozoic sedimentary grabens in the Western Carpathians' foreland (NE Bohemian Massif). *International journal of earthquakes, 104*(4), 963-990. http://doi.org/10.1007/s00531-014-1121-7

Štěpančíková, P., Stemberk, J., Vilímek, V., & Košťák, B. (2008). Neotectonic development of drainage networks in the East Sudeten Mountains and monitoring of recent fault displacements (Czech Republic). *Geomorphology, 102*, 68-80, http://doi.org/10.1016/j.geomorph.2007.06.016

Štěpančíková, P., Hók, J., Nývlt, D., Dohnal, J., Sýkorová, I., & Stemberk, J. (2010). Active tectonics research using trenching technique on the south-eastern section of the Sudetic Marginal Fault (NE Bohemian Massif, central Europe). *Tectonophysics, 485*(1-4), 269-282. http://doi.org/10.1016/j.tecto.2010.01.004

Štěpančíková, P., & Stemberk, J. Jr. (2016). Region of the Rychlebské Hory Mountains - Tectonically Controlled Landforms and Unique Landscape of Granite Inselbergs (Sudetic Mountains). In Migoń, P., Landscape and landforms of the Czech Republic, Book Series: World Geomorphological Landscapes. *Springer*, 263-276. http://doi.org/10.1007/978-3-319-27537-6_21

Ulrych, J., Ackerman, L., Balogh, K., Hegner, E., Jelínek, E., Pécskay, et al. (2013). Plio-Pleistocene basanitic and mellitic series of the Bohemian Massif: K-Ar ages, major/trace element and Sr–Nd isotopic data. *Chemie der Erde, 73*, 429-450. http://doi.rog/10.1016/j.chemer.2013.02.001

Ustaszewski, K., & Schmid, S. M. (2006). Control of preexisting faults on geometry and kinematics in the northernmost part of the Jura fold-and-thrust belt. *Tectonics, 25, TC5003*, 1-26. http://doi.org/10.1029/2005TC001915.

Vavryčuk, V., Bouchaala, F., & Fischer, T. (2013). High-resolution fault image from accurate locations and focal mechanisms of the 2008 swarm earthquakes in West Bohemia, Czech Republic. *Tectonophysics, 590*, 189-195. http://doi.org/10.1016/j.tecto.2013.01.025

Walczak, W. (1954). Pradolina Nysy i plejstocenskie zmiany hydrograficzne na przedpole Sudetow Wschodnich (The paleovalley of Nysa river and hydrographic changes in Eastern Foresudetic area during Pleistocene). *Polska Akademia Nauk, Instytut Geografii (Polish Academy of Sciences, Institute of Geography), Prace Geograficzne (Journal of Geology), 2*, 51 pp. (in Polish)

Walczak, W. (1970) Obszar przedsudecki. Dolny Śląsk. Cz. II – Obszar przedsudecki (The Fore-Sudetic area, Lower Silesia). *Państwowe wydawnictwo naukowe, Warszawa*, 415 pp. (in Polish)

Zedník, J., Pospíšil, J., Růžek, B., Horálek, J., Boušková, A., & Jedlička, P. (2001). Earthquakes in the Czech Republic and surrounding regions in 1995-1999. *Stud. Geophys. et Geod., 45*, 267-282. http://doi.org/10.1023/A:1022084112758

Ziegler, P. A. (1992). European Cenozoic rift system. In Ziegler, P. A. (Ed.), Geodynamics of Rifting, Volume I. Case History Studies on Rifts: Europe and Asia. *Tectonophysics*, *208*, 91-111. http://doi.org/10.1016/0040-1951(92)90338-7

Ziegler, P. A., & Dèzes, P. (2007). Cenozoic uplift of Variscan Massifs in the Alpine foreland: Timing and controlling mechanisms. *Global and Planetary Change 58*, 237-269. http://doi.org/10.1016/j.gloplacha.2006.12.004